MODELLING OF REACTIVE SEPARATION SYSTEMS

Antti Pyhälahti

MODELLING OF REACTIVE SEPARATION SYSTEMS

Antti Pyhälahti

Dissertation for the degree of Doctor of Science in Technology to be presented with due permission for public examination and debate in Auditorium Ke 2 at Helsinki University of Technology (Espoo, Finland) on the 2nd of December, 2005, at 12 o'clock.

Helsinki University of Technology

Department of Chemical Technology

Laboratory of Chemical Engineering and Plant Design

Teknillinen korkeakoulu

Kemian tekniikan osasto

Kemian laitetekniikan ja tehdassuunnittelun laboratorio

ABSTRACT

The first part of this study is concerned with setting up a reactive distillation process for production of tert-amyl-methyl ether (TAME). This work was linked to the development of etherification technology of Neste Oy. TAME production makes possible to upgrade some low value olefinic components to high value gasoline. Moreover, it has a significant impact in the reduction of the air pollution caused by the cars by introducing oxygen to the gasoline. However at the time of the study, there was no technology available for production of that component.

Reactive distillation (RD) had been applied successfully to the production of the tert-butyl-methyl-ether (MTBE). Thus it seemed worth of trying to apply RD to TAME production as well. The actual work of setting up the process was accomplished using a simulation model of a reactive distillation column. Arrangement of the column and conditions of the experimental runs were determined with the model developed earlier by Aittamaa and Kettunen (1993). The pilot run was successful, so that ethers could be produced as planned and experiments verified with the existence of the operating regimes predicted by the model.

The results of this study had a significant impact on the development of the highly successful NExTAME and NExETHERS technologies, even if the final solution was based on the Side Reactor Concept (SRC), i.e. a combination of a distillation column and a reactor connected to the column via side streams, rather than on RD.

The second part is the development of a rate-based model of a reactive distillation column including the effects of incomplete lateral mixing on the trays. Most published tests with RD have been performed with small pilot or bench scale columns. In such columns vapour and liquid mixing is nearly complete. However, that is not the case in large industrial columns.

On the other hand, making tests with reactive system in columns having diameter of two meter or more is very expensive and practically impossible for most research institutions. Not only the sheer size and utility consumption of such devices are large, but the feed and product volumes are huge even for a short run. With non-reacting systems it is often possible to recycle the products back to the feed, but when reaction takes place, that is much more difficult. If lateral mixing is suspected to have importance in some particular case, a mathematical model is probably the only viable way to estimate its significance before the full-scale plant is built.

Two different models for the effects of the lateral concentration profiles on reactive distillation trays were developed. The first model is an eddy diffusion model, the other one is a mixed pool model of reactive distillation trays. The basic principles of both models are known already earlier but both include novel features. Similar models have not been applied earlier to the reactive distillation.

The eddy diffusion equations are solved simultaneously and rigorously with the other equations of the equation group describing the column, instead of using solutions of strongly idealized problem as an approximation as has been usual with non-reactive distillation columns separating nearly ideal mixtures.

The mixed pool model differs from the ones presented earlier with its ability to take different mixing cases of the vapour phase into account. The normal assumption has been that the vapour is fully mixed between the column trays. Here is presented a simple and efficient method for treating columns with unmixed vapour flow from tray to tray. Two types of the liquid flow are considered – liquid flow to same direction on adjacent trays or liquid flow to contrary directions on adjacent trays.

In the third part a development of a combined model for SRC system is presented. When the SRC was found to be very useful in etherification processes, it was considered useful to develop a dedicated modelling tool for it. The part of the model describing the distillation column is in principle an equilibrium stage reactive distillation column model. The part of the model describing the side reactor(s) consists of a series of reactor segments. Each reactor segment is considered internally fully mixed, but using sufficient number of such segments in series, a plug flow reactor can be modelled with good accuracy. There is a significant flexibility in structure of the reactor sequence. The reactor system may operate in vapour or liquid phase or in co-current two-phase mode. Intercoolers or heat flows between surroundings and the reactor segments can be used.

As examples of the application of this model a case study of comparing SRC and RD in the production of tert-amyl-methyl-ether (TAME) and diisobutene is presented. The study showed that SRC optimisation of the reaction conditions is of crucial importance to the performance of the process. The developed model was proofed to be an efficient tool for this purpose.

The fourth part of this work was a part of development work of a novel tower packing by Sarvis Oy, The packing is continuously manufactured with the name HUFO. The results of the experimental work performed during the development project were used in order to develop an interfacial area correlation for a packed bed.

This correlation attempts to take the structural detail of the packing into account by introducing the width of the surface elements of the packing type into the correlation. In most correlations the specific surface and nominal size of the packing have been used for this purpose. However, the development of random packings has gone towards more and more heavily perforated shapes. The actual width of the packing walls interacting with the fluids in a bed consisting of some modern packing of certain nominal size is very different from the nominal diameter. Thus various correlations based on different combinations of the specific surface and of the width of the packing surface elements were tried. The best fit between the correlation and the test results was achieved when only the width of the surface elements was used in the correlation.

Another important result for practical chemical engineering is the observation that wettability of the plastic packing, known to be an important factor affecting the efficient interfacial area was greatly improved by the thin film of impurities deposited on the packing surface during the test program. The same thing may happen in industrial applications as well where impurities are common and run times long. Thus in many cases the efficiency correlations developed using brand new packings may be overly conservative.

PREFACE

The research described in this thesis was done in the Laboratory of Chemical Engineering and Plant Design in Helsinki University of Technology during 1990-2002.

The first part involving development of a reactive distillation process for etherification was done in cooperation with Neste Oy, supported by TEKES, the second part including the development of the hydrodynamic models of reactive trays was accomplished within the frame BRITE-EURAM Project Reactive Distillation (CEC Project No. BE95-1335). The third part, development of the distillation column – side reactor model was done in service of Neste Engineering Oy (Present Neste Jacobs Oy). The fourth part concerning interfacial area correlation for random packings was accomplished in cooperation with Aaltosen Tehtaat Oy / Sarvis.

Helsinki April 2005

Antti Pyhälahti

LIST OF PUBLICATIONS

This thesis is based on the following publications (Appendices I-VI), which are referred to in the text by their roman numerals:

I   Bravo J.L., Pyhälahti, A., Järvelin, H., Investigations in a Catalytic Distillation Plant: Vapour/Liquid Equilibrium, Kinetics and Mass-Transfer issues, *Ind. Eng. Chem. Res.* **32** (1993) 2220 – 2225.

II   Kenig, E.Y., Pyhälahti, A., Jakobsson, K., Górak, A, Aittamaa, J., Sundmacher, K., Advanced Rate-based Simulation Tool for Reactive Distillation, *AIChEJ*, **50**, (2004), 322-342,

III   Pyhälahti A., and Jakobsson, K., The Ratebased Mixed Pool Model of a reactive distillation column, *Ind. Eng. Chem. Res.* **42** (2003) 6188 – 6195.

IV   Jakobsson, K., Pyhälahti, A., Pakkanen, S., Keskinen, K., Aittamaa, J., Modelling of a Side Reactor Configuration Combining Reaction and Distillation, *Chem. Eng. Sci.* **57** (2002) 1521-1524.

V   Tuomas Ouni, Kaj Jakobsson, Antti Pyhälahti, Juhani Aittamaa, Enhancing Productivity of Side Reactor Configuration through Optimising the Reaction Conditions, *Chemical Engineering Research and Design* **82**(A2) (2004) 167-174.

VI   Pyhälahti, A., Järveläinen M., Correlations for interfacial area in a packed column, 1990, paper in CHISA '90 conference, 8 p.

Antti Pyhälahti's contribution to the appended publications

I   The paper is related to the Reactive Distillation project which was cooperation between Helsinki Univestiy of Technology and Neste Engineering Oy. In the project the author was responsible of simulation of the process and planning the test runs and writing of the manuscript together with the co-authors.

II   The paper is related to the BRITE-EURAM Project Reactive Distillation. In the project the author was responsible for developing and implementing the mass transfer and hydraulic correlations of the trays to the model. The section: "Modeling reactive tray hydrodynamics" is written almost exclusively by the author. In addition the author had a significant role in setting up the reactive distillation simulation program. Thus the author has participated to the model development, simulation and experimental planning and writing of the manuscript together with the co-authors.

III   The paper is also related to the BRITE-EURAM Project Reactive Distillation. The author has continued the development of the mixed pool model of a cross flow reactive tray, presenting the results here. The author has participated to the writing of the manuscript together with the co-authors.

IV   The author participated in the definition of research plan, modified the existing system of equations for a reactive distillation column so that it could be used for simulation of the reactor sequence. Most importantly this involved expanding the equation system of a reactive distillation column with equations representing the side reactor and outlining the arrangement of equations resulting in the Jacobian matrix structure presented in figure 4.5. Moreover the author participated to the programming of the model and participated to the writing of the manuscript.

V   The author has participated in the definition of research plan and participated to the generation of the examples, especially to those ones concentrating on the production of the isooctane.

VI   The paper is related to the development program of HUFO tower packing. In the project the author was responsible of planning the experiments, design and construction of the testing equipment, performing the tests, developing the correlations, reporting the results and writing the paper.

MODELLING OF REACTIVE SEPARATION SYSTEMS

1 INTRODUCTION

Predicting of the performance of process equipment belongs to the very foundations of the chemical engineering. Such predictions are necessary for e.g. the process development and design, determining the structure and the size of the new equipment or the evaluation of the existing equipment.

In the early history there was available very little other guidelines than experience gathered by trial and error when e.g. whisky distilleries where designed and constructed. However, with the development of the mathematical models describing the chemical thermodynamics and chemical processes and process equipment, such work is nowadays in large extent based on applying mathematical models. Thus mathematical models of the processes and various pieces of equipment belong to the most important tools of a chemical engineer. Moreover, developing of such models was one of the areas where chemical engineering science has its origin.

In spite of the long history, this field is by no means exhausted, but continuous introduction of new processes and new equipment together with improved modelling capabilities ensure that new models of chemical engineering hardware will be developed and the old models improved as long as the chemical engineering science is practised.

When a new process is developed, modelling is extremely useful. If necessary physical and chemical data exists, it is possible to evaluate a number of competing designs with a process simulator and select the most promising ones for experimental testing. Because the pilot testing is expensive and time consuming, it is a great advantage that resources needed for finding the optimal operating conditions can be reduced by simulation. This possibility is of special importance for reactive distillation, which combines distillation of often strongly non-ideal solutions to reactor design. Some of the questions to be answered are: what is the maximum capacity, how many stages are needed, which pressure to use, where the catalyst should be placed, how to distribute the feed, what will be the product composition?

These questions need to be addressed when a process around a reactive distillation column is designed, as matter of fact, already when a pilot plant is constructed. That can be accomplished by applying rules of thumb and a model of a reactive distillation column. The design developed by means of a simulation model still needs to be verified experimentally, but screening the alternatives in a computer instead of a pilot plant saves a lot of time and money. Also when the results are interpreted, the computer model gives insight to the inner workings of the process, which is very useful when it is further improved.

In many cases the most practical way of combining a reactor and a distillation column, is to combine a conventional distillation column and a conventional reactor to a side reactor arrangement instead of using a reactive distillation column. Such system can be modelled by combining a conventional distillation column with a conventional reactor with appropriate intermediate streams. However, solving such model is frequently tedious. Convergence can be improved and calculation time reduced using a special model solving the combined system including the column and reactor together with the intermediate streams simultaneously. Rapid convergence is of profound importance, when a process

optimisation is required and optimisation is of crucial importance when the SRC or RD is used.

The mass transfer performance of the cross flow trays is one of the most important factors of practical distillation column design. The distillation columns are frequently the most expensive and complicated devices of a chemical plant and even a slight improvement in the predictions over their performance would often result in significant savings. It is still a common practice that distillation column are designed using some rule of thumb about their average efficiency based on the experience of similar applications. However, sometimes those rules of thumb are in error resulting either in overdesign or unsatisfactory performance of the column. Especially problematic the situation is when a chemical reaction takes place on the trays. If there is no earlier experience of the same application, making any well-founded predictions without proper models is practically impossible.

Cross flow trays are probably the most usual type of mass transfer column internals. As the name says, characteristic to such a tray is that vapour liquid contacting happens in cross flow pattern. In spite of this, the vast majority of the existing distillation column models ignore this flow pattern. In many cases this simplification can be done, but in reactive distillation where reaction takes place and system is usually highly non-ideal, extrapolation of the behaviour of binary ideal mixture to the system at hand may lead to erroneous conclusions. Thus a more rigorous model of reactive cross flow trays has definitely value when new equipment is developed.

When a new type of tower packing is developed, during the development work itself theories and models of the functioning of the packing give guidelines to the development work. Also when development work itself is done and the new type is brought to the market, it is imperative for the manufacturer to be able to predict its performance. Otherwise it may be very difficult to find any company willing to buy such packing. Thus, testing of the new shapes and developing performance correlations for them is an essential part of the development work.

Efficient interfacial area is one of the key parameters in mass transfer over a phase interface. In spite of its importance, it is frequently not measured separately but as part of a combined mass transfer coefficients. One frequently applied method of testing tower packing is absorption of carbon dioxide into sodium hydroxide solution. This method is especially suitable for measuring efficient interfacial areas. This method was applied for testing the mass transfer performance of a number of novel plastic tower packing and from those results a correlation for interfacial area was developed.

2 TAME Production with Reactive distillation

2.1 Introduction

The study described in paper I was a co-operation between Helsinki University of Technology and Neste Oy. This work was related to the development of etherification technology of Neste Oy, which had already been ongoing for several years.

Lindqvist et al. (1996) have presented the history of the development of the etherification technology by Neste and a short summary is presented here to show the wider context of this work. The research of the etherification at Neste started in the end of 1970s, when the applicability of methyl tert-butyl-ether (MTBE) as a gasoline component was studied. A MTBE-unit was constructed to the Porvoo refinery in 1981. First studies concerning the tert-amyl-methyl-ether (TAME) production were performed in early 1980s. Significant progress in technological issues was achieved, but when the value of the product was based on octane value alone, the process was not profitable. In the second phase of TAME process development, the etherification of the reactive C6 components present in the gasoline fraction from a fluid catalytic cracking (FCC) unit was studied. Although the increase of the product volume was significant, that was not sufficient to make the process profitable. In the end of 1980s a novel ethyl-tertiary-butyl ether (ETBE) process was developed. The process was technically feasible, but the high price of ethanol made the process uneconomical.

Simultaneously the first model of the TAME-process was developed based on the kinetic measurements of Pavlova et al. (1981). In the early 1990s the basic research on catalytic distillation was carried out in cooperation with Helsinki University of Technology and the tests described in paper I are a part of this study. In 1991 two novel innovations related to the TAME process came through:

1) the use of C4/methanol azeotrope to eliminate the need for methanol washing

2) the use of side reactors

These inventions were a breakthrough that enabled the operation of a high conversion etherification plant without an expensive methanol recovery section.

In early 1990s demand for the renewable oxygenates increased. As a result tertiary amyl ethyl ether (TAEE) was included to the development program. In 1992 Neste started marketing of reformulated gasoline with 2% of oxygen. This made a drastic change to the profitability of the TAME and heavier ether process. When both octane increase and the oxygen content were taken into account, the profitability was very good. The NExTAME unit in Porvoo was constructed and started in 1995 and has been operating without problems ever since. During 1990s a combined process for MTBE, TAME and heavier ethers was developed and named NExETHERS. In recent years several etherification plants based on these technologies have been built.

2.2 TAME reaction system

The basic TAME formation reactions are:

$$CH_3OH + \text{2-methyl-1-butene} \leftrightarrow TAME \qquad (15)$$

9

$$CH_3OH + \text{2-methyl-2-butene} \leftrightarrow TAME$$
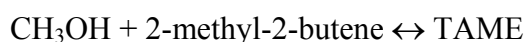
Most important side reactions are isomerisation of 2-methyl-1butene to 2-methyl-2-butene:

$$\text{2-methyl-1-butene} \leftrightarrow \text{2-methyl-2-butene},$$

formation of dimethyl ether and water from methanol:

$$2CH_3OH \leftrightarrow DME + H_2O,$$

formation of tertiary amyl alcohol (TAOH) from the isoamylenes:

$$H_2O + \text{2-methyl-1-butene} \leftrightarrow TAOH,$$

$$H_2O + \text{2-methyl-2-butene} \leftrightarrow TAOH,$$

and formation of dimer of the 2-methyl-butenes.

$$2\ (\text{2-methyl-1-butene}) \rightarrow C_{10}H_{20},$$

$$\text{2-methyl-1-butene} + \text{2-methyl-2-butene} \rightarrow C_{10}H_{20}$$

$$2\ (\text{2-methyl-2-butene}) \rightarrow C_{10}H_{20}.$$
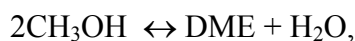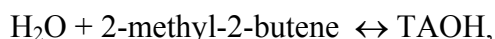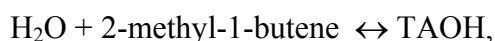
The reaction equilibriums and rates are different from that of MTBE. Thus it was necessary to develop a new process for producing TAME. The overall rate of the reaction is significantly slower than that of the MTBE reaction requiring larger catalyst amounts. Also the reaction equilibrium is less favourable than in the case of MTBE making impossible to achieve a high conversion in a single reactor train as was possible with MTBE.

2.3 Reactive Distillation Process for TAME production

The focus of the study presented in paper I is on the RD-process for TAME production. It was known that a very high conversion in MTBE production with RD is possible. Thus, it seemed natural to apply RD to the production of TAME, which is the next member of the homologous series of tertiary methyl ethers. Thereby the experiments described in the paper I are connected to the development of the etherification technologies of Neste. Later this development work resulted in NExTAME and NExETHERS-technologies, which are not based on RD. Nevertheless these tests were an important part of the development work, because they were the only available pilot results of the TAME production with RD.

On the process flow diagram level a reactive distillation process is very simple because most of the key operations, reaction and most important separations are combined to a single device. However, the complexity of the inner workings of a reactive distillation column itself is formidable. In the case of the TAME production, the reaction mixture has strongly non-ideal vapour-liquid equilibrium behaviour with methanol forming azeotropes with all other major components involved. Reaction takes place in a multistage counter-current cascade with simultaneous vapour-liquid mass transfer instead of single-phase operation of a conventional fixed bed reactor. The control of the process combines all the problems of complex multiphase reactor to those of the azeotropic distillation.

At the time when the project was started, Aittamaa and Kettunen (Kettunen1993) had already developed a simulation model for reactive distillation. This model is based on the

equilibrium stage approach. There was a kinetic model for TAME formation based on the data of Pavlova et al.(1981). As for the hardware, there was available a reactive distillation column in the synthesis pilot of Neste Oy. Thus, the most important tools for making a preliminary design for reactive distillation process were available and the work remaining was to set up the process itself.

Extensive simulation work resulted in the column arrangement presented in figure 3.1 with hydrocarbon entering to the lower feed point and additional methanol being fed either with the C5 feed of through the upper feed points. Suitable feed rate and process conditions for this system were estimated as well.

In principle the purpose is to operate the column so that the reactants reside mainly in the catalytic section of the column. Reaction product is heavier than the reactants and it is removed via the the bottom stream. The remainig unreacted material is removed with the distillate stream.

Although the principle is simple, the properties of the system cause a number of complications. Methanol forms an azeotrope with C5-hydrocarbons containting about 20% of methanol. Thus it is necessary to feed to the system enough methanol both to have the azeotropic concentration at the top in addition to the amount consumed in the reactions or the methanol concentration in the middle part of the column will be very low.

On the other hand, the proper amount should not be exceeded much because the portion of unreacted methanol which exceeds the amount needed to establish the azeotropic composition at the top, will end up to the bottom product, i.e. into the TAME product. Ideally there should be just enough of excess methanol to keep a high methanol concentration in the upper part of the column up to the lower end of the catalytic part of the column, but only minimal amount should appear in the bottom product. Thus correct methanol feed rate is one of the key factors for the good operation and it should be set accurately.

Figure 2.7 presents the summary of the results of a sensitivity study of the methanol feed rate in a reactive distillation column producing TAME. The abscissa of the figure is the methanol feed rate to the column and 100 % corresponds to the optimum value of the feed rate. Ordinate is the TAME yield based on the total amount of 2-methyl-1-butene and 2-methyl-2-butene present in the column feed. As can be seen, the maximum yield under the simulated conditions is about 80%, which is a relatively high figure for a TAME process involving only a reactive distillation column. Unfortunately the optimum point is a sharp peak and deviation from it will cause a rapid deterioration of the yield. Especially the loss of yield based on the methyl-butenes when methanol feed is increased may appear counterintuitive. However, it must be kept in mind, that in a reactive distillation column feed rates do not directly determine the concentrations prevailing in the catalytic zone of the column. Feed rates, product draw rates and reflux rate must be carefully matched with each other in order to establish the optimum conditions.

If the feed rate and composition are very steady, it is conceivable that the conditions can be optimised. However, in a normal refinery environment the fluctuations of the feed rate and composition are commonplace and optimal adaptation to them is difficult.

Selection of the optimal methanol feed point is a good illustration of the complex vapour liquid equilibrium of the system. Optimal methanol feed location depends on its concentration in the catalyst zone. If methanol concentration in the catalytic zone is kept below the azeotropic, methanol behaves as a light component and tends to rise upwards. In that case methanol should be fed below the bed with the hydrocarbon feed, because methanol fed to the upper feed points will not descend to the lower parts of the catalytic section. On the other hand, if the column is operated at a high methanol mode, it is better to feed methanol above the catalyst beds, because then it behaves as a heavy component and moves downwards. Under such conditions it is possible to exceed the azeotropic concentration of methanol in the liquid phase at the upper end of the catalyst bed. The methanol feed rate must be carefully matched to the amount consumed by reactions and carried away by the C5-methanol azeotrope, for the optimal production conditions.

2.3 The Experiments

The test runs reported in paper I were set up more to test the validity of the simulations and the existence of the operating regimes detected than to represent the optimal production conditions. Correspondingly the sequence of the experimental conditions was selected to cover a wide range of methanol/hydrocarbon feed rates. Methanol feed point was changed as well.

The system was started with a high methanol feed rate. Then the methanol feed rate was gradually reduced until the methanol concentration profile was low.

The run was arranged so that after the initial stabilisation the first set of samples was drawn. Then the conditions were changed and system was allowed to stabilize overnight and the next set of samples was taken. Thus there was approximately 23 hours stabilization time between the experimental points, which was estimated sufficient based on the system hold-up and flow rates and verified with flow and temperature measurements.

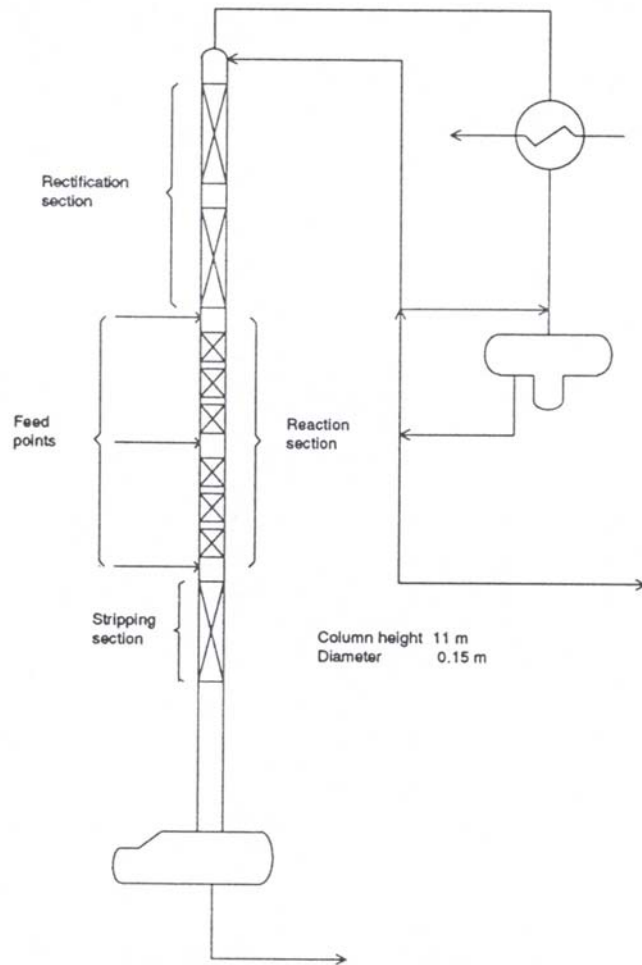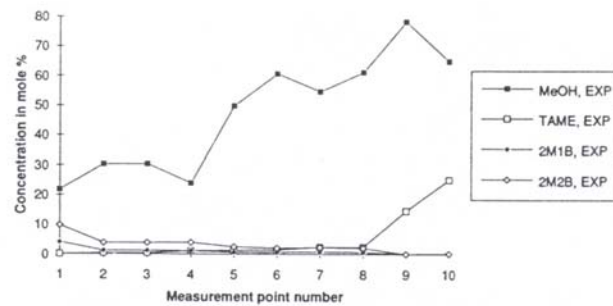Figure 2.1. The pilot column used in reactive distillation experiments

Figure 2.2. Experimental concentration profiles with high methanol feed rate
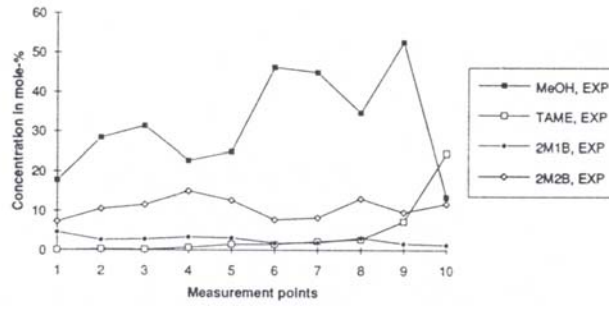
Figure 2.3. Measured concentrations with medium methanol feed rate
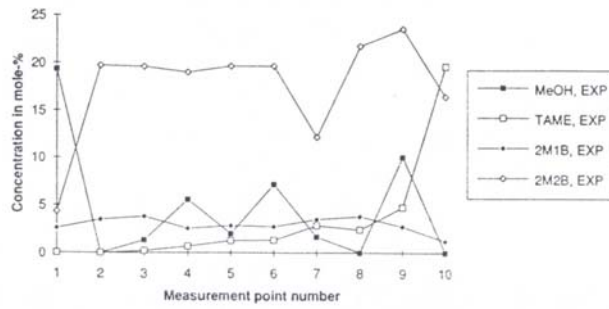
Figure 2.4. Measured concentrations with low methanol feed rate
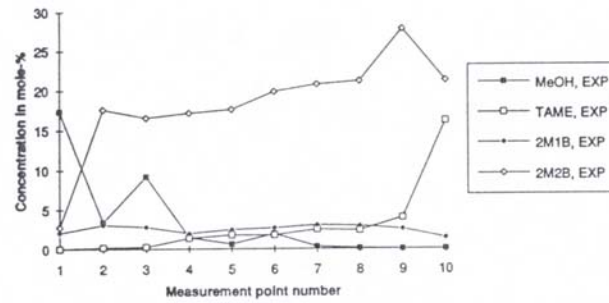
Figure 2.5. Measured concentrations with low methanol feed rate
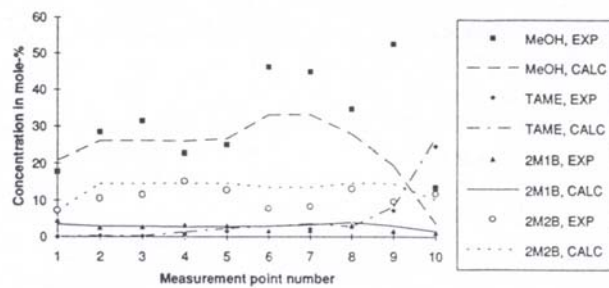
Figure 2.6. Comparison of predicted and measured composition profiles.

14
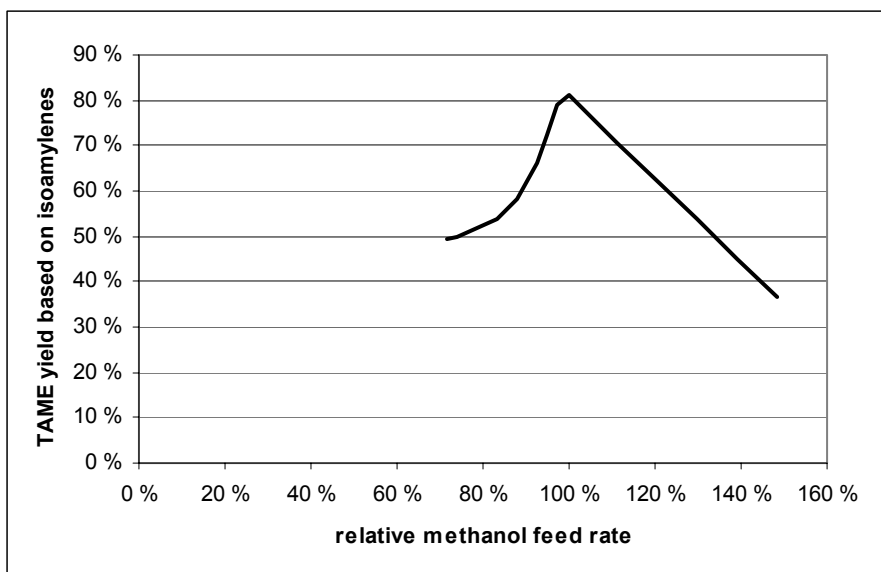
Figure 2.7. The simulated TAME yield as a function of the methanol feed rate in a reactive distillation process. On the x-axis is shown the relative methanol feed rate so that 100% corresponds to the optimum feed rate.

2.4 The Discussion of the results

Figures 2.2-2.5 present column concentration profiles with various levels of methanol feed rates. Figure 2.6 presents comparison between the simulated and experimental concentration profiles

The experiments verified fully the existence of the predicted operating regimes The column operated in tests as expected although the models in the time of making the study were by no means perfect. The methanol concentration at the column top corresponds to the azeotropic and at high methanol feed rate the methanol concentration tends to increase towards the column bottom. When methanol feed rate is reduced, the concenration at the column top remains about constant, but the concentration at the lower parts of the column is gradually reduced when the amount of excess methanol decreases.

There was a deviation between the experimental and simulated results as can be seen in figure 2.6. In the simulation model used for generating the calculated points in figure 2.6 the parameters were not specifically adjusted according to the results beyond setting the feed streams, reflux rate and product rate to the values prevailing during the experiment.

Differences were due to the experimental errors as well as the inaccuracies of the models. An additional reason of discrepancy may be that the time needed for establishing the steady state in a reactive distillation system was underestimated. The process dynamics of

the reactive distillation column treating an azeotropic mixture is complicated, and the normal rule of thumb of 3-6 times the residence time being a sufficient stabilisation period may have failed. This may have resulted also in suspecting of encountering multiple steady states, which are mentioned in paper I. The large difference of the methanol concentration at point 9 in figure 2.6 is likely to be an analysis error.

As a process for TAME production, RD was found to be feasible, but better alternatives were found. The best properties of RD are obviously related to fast, heavily equilibrium restricted reactions with such VLE-properties that operation resembling that of an counter-current absorber can be established. With TAME the reaction equilibrium is less favourable than with MTBE but still the equilibrium is typically well above 50%. On the other hand, reaction is relatively slow requiring large amounts of catalyst. Placing large volumes of catalyst inside a distillation column is uneconomical because large part of the volume must be reserved for the two phase flow in any case. When reaction takes place in the liquid phase, the fact that the reactants are more volatile than the reaction product is an additional drawback. In this case catalyst is present in the phase rich in reaction products and lean in reactants.

Moreover, due to the azeotropic character of the VLE system it is difficult to arrange the methanol feed in an optimal way under varying conditions as is illustrated by the result presented in figure 2.7, and so that a very high conversion of all reactants could be achieved simultaneously. If a pre-reactor, where major part of the reactants are consumed, is placed in front of a RD column, the problem is much easier, because less methanol needs to be fed directly to the column. In such arrangement RD is used only as a polishing stage and theoretically it is possible to achieve a very high isoamylene conversion. However, in practice very high isoamylene conversions (>90%) are seldom required. Additionally, placing catalyst inside the column requires complicated and expensive internals and if catalyst is damaged, replacing it requires usually a shutdown of the plant. The conclusion was that RD was possible and superior technology for TAME-production but even better technology was developed later.

3 Tray hydrodynamic models

3.1 Introduction

One of the targets of the studies presented in papers II and III was to provide a rigorous rate-based cross-flow model for a reactive distillation column.

The concentration distribution on a cross flow tray is not even. The flow pattern of the liquid on the tray influences the mass transfer and reaction rates on a distillation tray. The vapour concentration changes gradually when it rises through the liquid on the tray. The liquid concentration also changes gradually from the inlet to the outlet of the tray.

There are several ways to model the concentration distributions on a distillation tray. Vapour and liquid may be considered fully mixed vertically and horizontally. This is the approach for both the traditional equilibrium stage models and the standard rate-based model (see, e.g., Taylor and Krishna, 1993). This approach can be improved by assuming that in the vertical direction the vapour is flowing in a plug flow through the liquid (Taylor and Kooijman, 1995). Vertical liquid concentration gradients are likely to be small due to

the intense mixing due to the vapour flow through the liquid. Nevertheless, Higler et al. (1999) have presented a multicell model taking the vertical concentration gradients in the liquid into account.

In the horizontal direction on the vapour side, it may be assumed that either vapour is totally mixed before it enters the tray or that after being separated from the liquid on the tray below, the vapour does not mix at all. The real situation is obviously between these two limiting cases.

Horizontal liquid flow pattern is complex due to the mixing by vapour, dispersion and the round cross section of the column. A rigorous modelling of this flow pattern is very difficult and frequently the situation is simplified by assuming that the liquid flow is unidirectional and the major deviation from the plug flow is the turbulent mixing or eddy diffusion.

In the studies presented in papers II and III two modelling approaches were used. The first one is a modification of the eddy diffusion or the backmixing model, the other one is a modification of the mixed pool model.
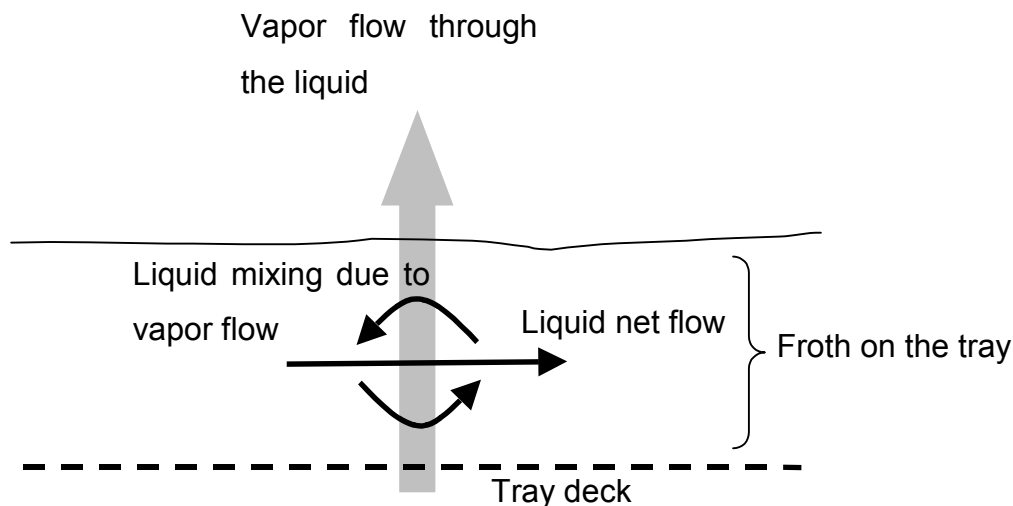
Figure 3.1 Flows and lateral mixing of the liquid on a cross flow distillation tray.

3.2 Rate-based eddy diffusion model model of a reactive distillation column

3.2.1 The model structure

This model is described in paper II, section: *the eddy diffusion model.*

The schematic presentation of a point on the tray is presented in Figure 3.1. Assuming that the flow is one dimensional, the liquid is completely mixed within the plane perpendicular to the direction of the flow, and that the condition of the entering vapour is constant throughout the tray, the basic steady state eddy diffusion equations for the components and enthalpy can be written as follows:

$$-c_t D_e w h_f \frac{\partial^2 \mathbf{x}(l)}{\partial l^2} - \frac{\partial(L(l)\mathbf{x}(l))}{\partial l} + \mathbf{N'}(l) + \mathbf{R'}(l) = \mathbf{0} \qquad (3.1)$$

$$-c_t D_e w h_f \frac{\partial^2 H^L(l)}{\partial l^2} - \frac{\partial(L(l)H^L(l))}{\partial l} + E'(l) = 0 \qquad (3.2)$$

Here $\mathbf{N'}(l)$, $\mathbf{R'}(l)$ and $E'(l)$ are the specific mass transfer rate vector, reaction rate vector and heat transfer rate per unit length of the tray at distance l from the exit weir, respectively. There is no specific term form heat of reaction in equation 3.2 because in the the heat of formation was included to the component enthalpies.

Formally the eddy diffusion equation is similar to the corresponding molecular diffusion equation. However, the eddy diffusivity coefficient depends only on the flow conditions on the tray and thus is the same for all components. There are several experimental correlations available in the literature for evaluating the eddy diffusion coefficients.

Because the equations 3.1 and 3.2 are second order differential equations, they need two sets of boundary conditions. Those are selected by an analogy to the conditions applied to the non-reactive trays (Gerster et al., 1958).

The purpose is to model trays with catalyst present on the tray deck, thus reactions will stop together with the mass transfer when liquid passes the outlet weir. With this assumption, the source term due to reaction is formally similar to the source term due to mass transfer in equation 3.1 and the argumentation concerning the boundary values on the non-reactive trays can be extended to this case, too. The selected boundary conditions are that the outlet condition must be at the value set by the overall tray material and energy balances (equation 3.3) and the concentration and temperature gradients at the outlet weir are negligible (equation 3.4):

$$\mathbf{x}\big|_{l=0} = \mathbf{x}_k \qquad (3.3)$$

$$\frac{d\mathbf{x}}{dl}\bigg|_{l=0} = \mathbf{0} \qquad (3.4)$$

The boundary conditions of the enthalpy are defined by analogous equations. The equation 3.3 is easy to understand, but the equation 3.4 is not as self-evident. From the assumption that the catalyst is not present outside the active bubbling area follows that the reactions will stop when liquid leaves the tray. Mass transfer will stop simultaneously. Thus at negative l values corresponding to points beyond the outlet weir, it seems natural to assume that there is no concentration gradient. On the other hand, if there would be a finite concentration or temperature gradient at very small positive l values, there would be a finite mass or heat transfer to or from the outlet weir due to diffusion. This mass transfer would come to an abrupt end at $l=0$, because the gradient was assumed to vanish beyond that point and thereby mass transfer due to eddy diffusion (or molecular diffusion as well) would cease. This discontinuity would result in a step change in the liquid concentrations and temperatures, which seems not a reasonable physical condition. This discontinuity is avoided by setting the concentration and temperature gradient to zero at the outlet weir by equation 3.4.

The independent variables for each tray are:
- L, liquid flow rate

- x_i, $i=1...n$ liquid mole fractions
- H^L liquid enthalpy
- p pressure
- H^V vapour enthalpy
- y_i, $i=1...n$ vapour mole fractions
- V vapour flow rate.

The liquid variables are taken at the liquid outlet conditions and the vapour variables at the average conditions of the vapour leaving from tray.

The total number of the independent variables and equations is apparently reduced substantially from that of an equivalent rate-based model, i.e. from $5n + 6$ to $2n + 5$ in the current model. A striking difference is that the equation group contains only the heat and material balances and the pressure specification but not any equilibrium or mass transfer rate equations. The pertaining variables assuming discrete values in the completely mixed liquid model are in this case replaced by continuous functions and thus cannot be treated as single numbers. Thus the system of equations describing the column is written as a system of integral equations containing the following items for each tray:

- vapor total mass balance

$$0 = -G_k - S_k^G + G_{k-1} - \sum_{i=1}^{n}\left[\int_0^{l_f} N'_{i,k}(l)dl\right] + \sum_{i=1}^{n} F_{i,k}^G \tag{3.5}$$

- vapor component mass balances

$$0 = -\left(G_k + S_k^G\right)y_{i,k} + G_{k-1}y_{i,k-1} - \int_0^{l_f} N'_{i,k}(l)dl + F_{i,k}^G \quad ; \qquad i = 1,...,n \tag{3.6}$$

- vapor enthalpy balance

$$0 = -\left(G_k + S_k^G\right)H_k + G_{k-1}H_{k-1} - \int_0^{l_f} E'_k(l)dl + \sum_{i=1}^{c} F_{i,k}^V H_k^F, \tag{3.7}$$

- liquid total mass balance:

$$0 = L_{k+1} + \sum_{i=1}^{n} F_{i,k}^L + \sum_{i=1}^{n}\left[\int_0^{l_f} N'_{i,k}(l)dl\right] + \sum_{i=1}^{n}\left[\int_0^{l_f} R'_{i,k}(l)dl\right] - L_k + S_k^L \tag{3.8}$$

- liquid component mass balances

$$0 = L_{k+1}x_{i,k+1} + F_{i,k}^L + \int_0^{l_f} N'_{i,k}(l)dl + \int_0^{l_f} R'_{i,k}(l)dl - \left(L_k + S_k^L\right)x_{i,k} \quad ; \qquad i = 1,...,n \tag{3.9}$$

- liquid enthalpy balance

$$0 = L_{k+1}h_{k+1} + \left(\sum_{i=1}^{n} F_{i,k}^L \right) h_k^F + \int_0^{l_f} E_k'(l)dl - \left(L_k + S_k^L \right) h_k \qquad (3.10)$$

- pressure drop equation

$$0 = p_k - \left(p_{k+1} + \Delta p_{k+1}^{spec} \right) \qquad (3.11)$$

Here the subscript k refers to the tray and the subscript i to the component.

According to the selected model, the variation of the concentrations and enthalpies of the liquid and vapour on the tray are governed by the eddy diffusion equation 3.1 and 3.2.

The integral terms present in the equations above are evaluated by solving the systems of differential algebraic equations (DAE) for the plates. This DAE system contains the following equations for each tray (the signs of the differentials result from the integration against the flow direction):

- differential equation for the total liquid flow (eddy diffusion does not produce a net flow):

$$\frac{dL_k}{dl} = - \left(\sum_{i=1}^{n} R'_{i,k} + \sum_{i=1}^{n} N'_{i,k} \right) \qquad (3.12)$$

- $n-1$ differential equations for the liquid mole fractions

$$\frac{d^2 x_{i,k}}{dl^2} = - \frac{1}{c_t D_e wh_f} \left(L_k \frac{dx_{i,k}}{dl} + x_{i,k} \frac{dL_k}{dl} + N'_{i,k} + R'_{i,k} \right) ; \qquad i = 1,...,n-1 \quad (3.13)$$

- differential equation for the liquid enthalpy

$$\frac{d^2 H_k^L}{dl^2} = - \frac{1}{c_t D_e wh_f} \left(h_k \frac{dL_k}{dl} + L \frac{dH_k^L}{dl} + E_k' \right) \qquad (3.14)$$

- equation for the sum of the liquid mole fractions

$$0 = 1 - \sum_{i=1}^{n} x_{i,k} \qquad (3.15)$$

- vapor total mass balance

$$0 = G_{k-1} - \left(\sum_{i=1}^{n} N'_{i,k} - G'_k \right) l_f \qquad (3.16)$$

- vapor-side enthalpy balance

$$0 = H_{k-1}^V G_{k-1} - E_k' l_f - H_k^V G_k \qquad (3.17)$$

- vapor side component mass balances:

$$0 = y_{i,k-1} G_{k-1} - N'_{i,k} l_f - G'_k \, y_{i,k} l_f \quad ; \qquad i = 1,...,n \tag{3.18}$$

- mass transfer equations

$$0 = N'_{i,k} - N^{calc}_{i,k} \quad ; \qquad i = 1,...,n \tag{3.19}$$

- equation for the sum of the equilibrium vapor mole fractions

$$0 = 1 - \sum_{i=1}^{n} y^*_{i,k} \tag{3.20}$$

- vapor-liquid equilibrium conditions

$$0 = K_{i,k} x_{i,k} - y^*_{i,k} \quad ; \qquad i = 1,...,n \tag{3.21}$$

The local heat and mass transfer rates per unit length (E' and $\mathbf{N'}$) at the distance l from the liquid outlet edge are calculated using the mass transfer correlations for appropriate types of trays involved. The local mass transfer model is similar to the rate based vapor plug flow model as presented by Taylor et al. (1994).

This method is based on the overall mass transfer coefficient matrix and thus does not require estimation of the interfacial conditions explicitly. This reduces the number of the necessary independent variables. However, any solution based on the overall vapor-side mass transfer coefficients requires the composition of the vapor phase in equilibrium with the liquid on the tray, in order to evaluate the mass and energy fluxes (see, e.g. Sherwood et al., 1975, Taylor and Krishna, 1993). This is the reason for including Eqs.3.20 and 3.21 into the governing system.

It is worth noting that the principal thermal variable in the DAE system is the liquid enthalpy, rather than the temperature. The main reason is that evaluation of the differential of the enthalpy is much easier than that of the temperature because the former results directly from the energy balance, whereas the latter is a complex function of system properties.

3.2.2 Solving the equations

The values of the mass and energy transfer and reaction rate terms in integral balance equations depend on the second order differential equations. Thus the whole equation system consists of group of integral and differential equations posing a considerable challenge for the solution.

The solution of the system of mass and energy balance equations is performed using a block tri-diagonal Newton method. The evaluation of the integral terms present in the balance equations is accomplished by solving the DAE system of the eddy diffusion equations of the tray using the current values of the independent variables as necessary initial values. During the solution of the DAE-equation system, the values of $\mathbf{N'}$, $\mathbf{R'}$ and E' are integrated over the whole flow path across the tray.

The initial values were generated by solving the problem first by setting the diffusion coefficient to a very large value corresponding to a complete mixing of liquid. Then diffusion coefficient was gradually reduced to the correct value.

3.2.3 Results of MTBE production

The model has been applied to some test systems. The column of the test is a pilot-scale reactive distillation column involving MTBE-reaction. It has 20 stages including condenser and reboiler. Reactions take place in the reactive section on the trays 8-13. The simulation involves four components, methanol, isobutene, methyl-tert-butyl-ether (MTBE) and isobutane. The reaction equation is:

$$MeOH + isobutene \leftrightarrow MTBE \qquad (3.22)$$

Isobutane does not react. The the reactive trays are treated as cross flow trays with catalyst placed as an even layer on the reactive trays.

The calculated concentration profiles of MTBE on the reactive trays of a pilot scale reactive distillation column producing MTBE are presented in figure (3.2). As can be seen from Figure (3.2) the concentrations vary significantly over the tray compared to the difference between the trays. E.g. the average MTBE mole fraction on tray 12 is approximately 0.0109 and on the tray 13 about 0.0065. Thus the difference is approximately 0.0044. On the other hand, the MTBE mole fraction on tray 13 varies from 0.00688 to 0.00581. Thus, in this case the change over the tray is approximately 25% of the change from tray to tray. However, it was noticed that the effect to the column overall material balance is negligible.
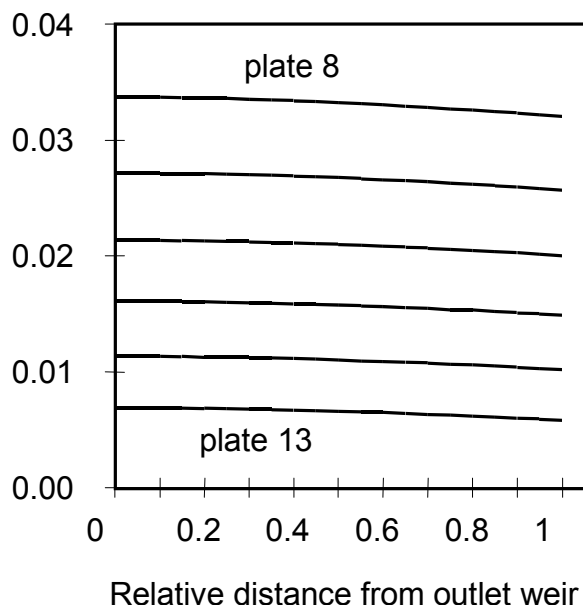

Figure 3.2 The calculated MTBE concentrations on the reactive trays.

3.3 Rate-based mixed pool model of a reactive distillation column

3.3.1 Model
The mixed pool model presented here differs mainly from the approach by Higler et al. (1999) by implementing various vapour mixing cases whereas Higler assumed complete vapour mixing between the trays. On the other hand, liquid is not divided vertically into layers as in the model of Higler et al. (1999), thus resulting in fewer model equations.

The vapour mixing cases presented by Lewis (1936) are applied here to a mixed pool model. Here we apply the nomenclature based on these cases: Lewis case 1 means total vapor mixing, Lewis case 2, is the case with unidirectional liquid flow on adjacent trays and Lewis case 3 with liquid flow changing direction on each adjacent tray without lateral mixing of vapour. These cases are presented in figure 3.3.
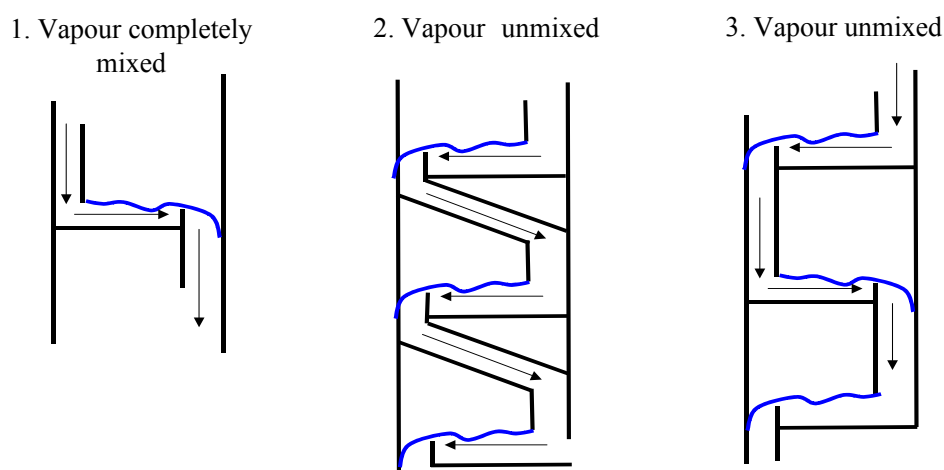
Figure 3.3 The various vapor mixing cases. From left ot right the Lewis cases 1 through 3

In a mixed pool model, case 1 can be simulated by combining all vapor flows rising from one tray, calculating the average composition and enthalpy of the combined stream and distributing this flow to the pools of the next tray. Case 2 can be approximated by connecting the vapor flow from the first cell of the lower tray to the first cell of the tray above etc. until the last pair of cells on each tray. Case 3 is approximated the same way but the cells are connected so that the first pool of the lower tray is connected to the last cell of the tray above etc.

Computationally this is a cheap way to model the Lewis cases 2 and 3. A slight complication over the case 1 results from necessity to compensate for uneven vaporisation or condensation in different areas of the tray, but that has no significant effect on the total computation effort needed.

In Figure 3.4 the division of the tray into mixed cells is presented. The case corresponds to the Lewis case 3. Thus, vapour is assumed to flow unmixed from each cell to the corresponding cell on the upper tray and liquid is flowing to opposite directions on the adjacent trays so that the liquid entering the tray is contacted first with vapour from the outlet side cell of the tray below. This is the normal flow pattern with cross flow trays.
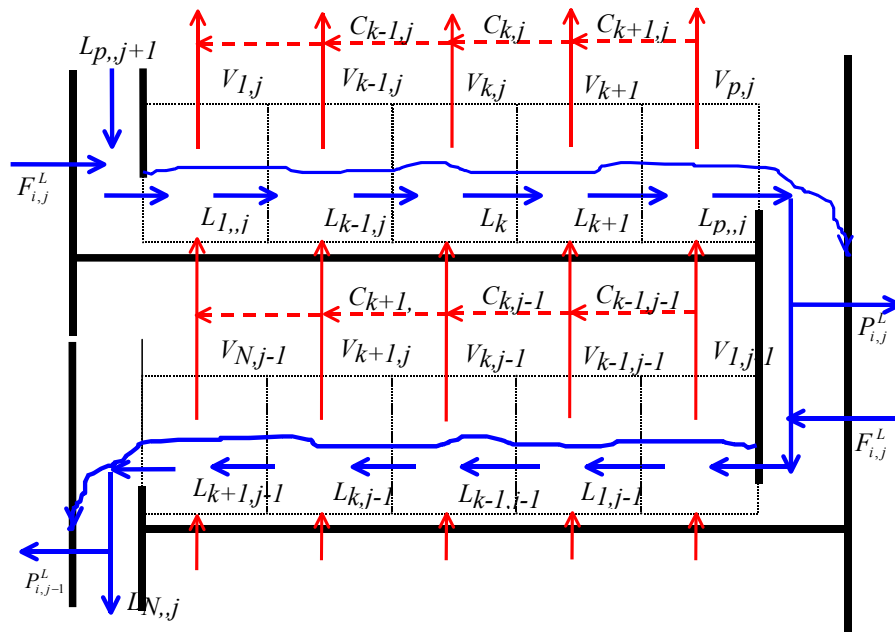
Figure 3.4. The mixed pools of a distillation tray when vapor is unmixed and liquid flows to contrary direction on adjacent trays (L liquid flow, V vapour flow, C vapor flow correction factors, F liquid feed flow, P liquid product flow).

Each pool or the mixed pool model has essentially the same variables and equations as the whole tray in the rate-based model assuming complete liquid mixing on each tray. The only deviation is that the pressure is assumed to be constant throughout the plate. Thus, if the number of mixed pools is u and number of components is n, there are $5un+5u+1$ variables on a tray instead of $5n+6$ of the fully mixed rate-based stage. The appropriate number of pools can be determined using the correlations of Ashley and Haselden (1970) and Alejski (1991). The liquid is assumed to be completely mixed in the direction perpendicular to the flow direction.

The independent variables for each tray are:
- u liquid flow rates
- $u \times n$ liquid mole fractions
- $u \times n$ liquid mole fractions at the interface
- u liquid temperatures
- u interfacial temperatures
- $u \times n$ mass transfer fluxes
- pressure
- u vapour temperatures
- $u \times n$ vapour mole fractions at the interface
- $u \times n$ vapour mole fractions and
- u vapour flow rates.

The corresponding equations to be solved are:
- u liquid-side total mass balances

- $u{\times}n$ liquid-side component mass balances
- $u{\times}(n\text{-}1)$ liquid-side mass transfer equations
- u liquid-side interface concentration summation equations
- u liquid-side energy balances
- u interfacial energy balances for each pool
- $u{\times}n$ interfacial equilibrium equations
- 1 pressure drop condition
- u vapour-side energy balances
- u vapour-side interfacial concentration summation equations
- $u{\times}(n\text{-}1)$ vapour-side mass transfer equations
- $u{\times}n$ vapour-side component mass balances and
- u vapour-side total mass balances.

The reboiler and condenser of the column are modelled as equilibrium stages. A more complete presentation of these equations is included to the paper III

To model the mass transfer in each pool, it is possible to use either the mixed liquid - mixed vapour or the mixed liquid - plug flow vapour model. The former model is based on the model presented by Taylor and Krishna (1993) whereas the latter model has its origin in Taylor et al. (1994). Both models have been modified by adding the reaction terms to the material balances. In addition, there are two modifications of the latter model, one of those based on the leaving vapour composition and the second based on the entering composition.

Pressure drop calculation is based on averaged flow rate and compositions.

3.3.2 Solver

The mixed pool model was solved using Newton's method with a block tridiagonal Jacobian matrix with numerically calculated derivatives. The implementation of the solver to this problem posed no special problems, but it was noticed that very heavy damping of the correction steps was necessary in order to keep the solution on the convergence path.

Newton method converges well when initial values are good. However, initialisation of the variables is of crucial importance for a problem of this complexity. The initial values were generated by solving the model first with each tray as a single mixed cell and the resulting concentrations, temperatures etc were used as initial values for the multiple cell mixed pool model.

3.3.3 Test example 1

The test case 1 is the same as the one used with the eddy diffusion model above. However, this time the simulation was done using the mixed pool approach.

This test case was simulated using seven different flow models. The case 1 was a mixed liquid-mixed vapour model without division to cells. Case 2 was a mixed liquid-vapour plug flow model without division to cells. Case 3 was a mixed pool model otherwise exactly identical with case 1 but with 4 cells per stage and with complete vapour mixing between the trays (Lewis case 1). Case 4 was otherwise identical to the case 2 but with each tray divided to 4 cell and with complete vapour mixing between the trays. The cases 5, 6 and 7 applied to this problem were mixed pool models with 5 cells per tray and with

vapour flow patterns corresponding to the Lewis cases 1, 2 and 3 respectively. In Figure 3 are presented the calculated molar fractions of MTBE on the reactive trays 8-13 with the case 3 (mixed vapour-mixed liquid, 4 cells per tray).

From Figure 3.5 it can be observed that there is a significant composition gradient of the reactive component along the flow path of the tray. The results are very similar to those ones achieved with the eddy diffusion equation above but the graphs are in this case step functions instead of the smooth curves produced by the eddy diffusion model. This result is naturally to be expected because both models were applied to the same case.

It was interesting to observe that the composition profiles in the column as well as in the product streams were almost identical in all calculated cases.
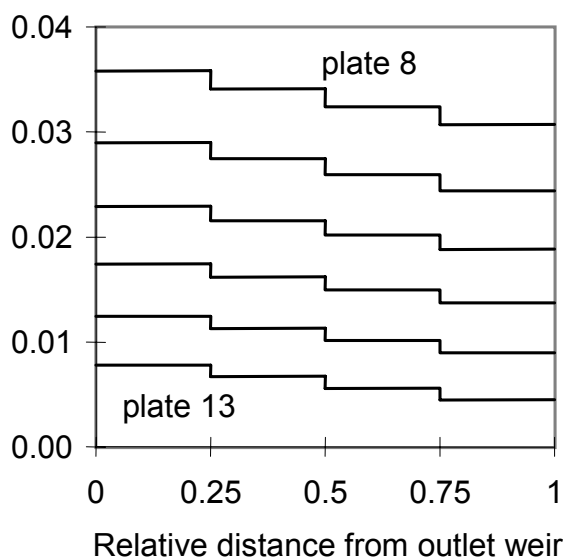
Figure 3.5. Mole fractions of MTBE along the flow path of the reactive trays in example 1, with complete vapour mixing between the stages

3.3.4 Test example 2

It is probable, that the lateral concentration variation is most significant when the number of trays is small and heat effects are large so that the variations of the flow rates and concentrations on the individual trays cannot cancel out each other. For testing this hypothesis another test case was set up. The column consisted of only six stages: reboiler, lower feed stage, two reactive stages, upper feed stage and condenser. Heat of reaction should be high, thus the MTBE-system of example 1 was modified so that the reaction enthalpy was increased by 150 kJ/mol. The isobutene-isobutane mixture enters from lower feed tray and methanol from upper feed tray but feed mixture is much more concentrated containing 50% of isobutene.

The results achieved using the mixed liquid-mixed vapour model with 5 mixed cells per stage and with complete vapour mixing between the stages is presented in table 5. The

reference case, otherwise identical, but without division to mixed cells is presented in table 6. The effect of tray scale phenomena is very significant. The reaction rate achieved with reference model in this case is approximately 1.3 mol/s, whereas according to the mixed pool model the reaction rate is only 0.7 mol/s. The distribution of the components between bottom product and distillate is clearly different. This example is artificial, but it illustrates under what kind of conditions the lateral gradients on the stages may be important. Such conditions are more likely to occur in a reactive absorber than in a distillation column.
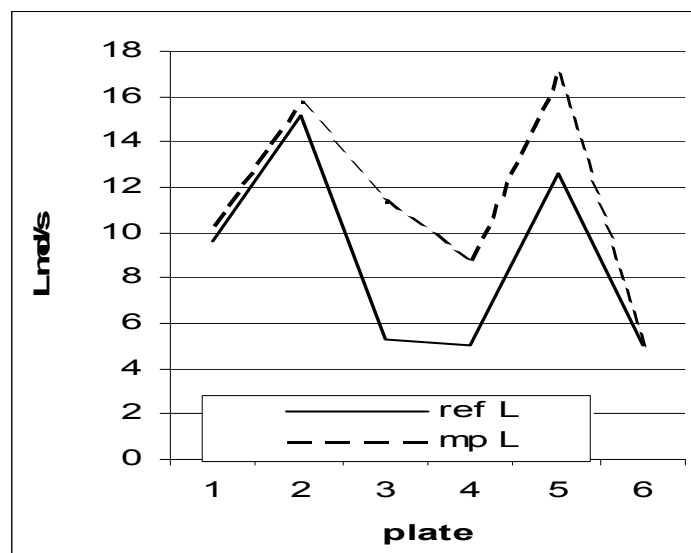
Figure 3.6. Liquid streams (mol/s) leaving the stages in example 2. (ref L reference calculation with each tray as a single cell, mp L calculated with 5 mixed cells per tray).

3.4 Discussion

Two models taking lateral concentration variation on reactive cross-flow trays are developed. Both model have been applied to test problems and have been solved successfully.

However, it was noticed that in a relatively tall distillation column the variation of the liquid compositions on the trays has very little effect on the overall performance independently of the modelling method applied.

Obviously, if the reaction and mass transfer rates change in one part of the system, this change tends to result in opposite change on adjacent plates. E.g, if reaction rates increases on certain plate, the result is that there is less reactants present on the adjacent trays resulting in lower reaction rates on those trays. Thus the overall effects tend to cancel out each other.

The lateral concentration gradients are likely to have largest effects on large diameter column having small number of trays so that the neighbouring trays cannot compensate the changes.

This hypothesis was tested by creating a test case involving a highly exothermal reaction in a short column. In that case the total reaction rate dropped by approximately 45% when the fully mixed liquid model was replaced with a mixed pool model.

27

The worst drawback of both of the models presented here is the significant increase of the calculation time. With the mixed pool model, the increase of the time needed for taking one Newton step is approximately proportional to the square of the number of equations of one tray. There was no significant difference between various vapour flow cases. With the eddy diffusion model, the number of independent variables and equations is reduced significantly but discrepancy functions involve differential and integral equations making their evaluation with a DAE-solver tedious.

The current industrial catalytic distillation packings do not follow the cross flow pattern, which is the basis of these models The distillation column internals involving solid catalyst are mainly various catalytic packing types and they work principally in counter-current mode. One of the results of this study is that development of such packings for MTBE-production seems not to be profitable.

In a trayed absorption column the may be very different. If reaction takes place in the liquid either without catalyst or is homogeneously catalysed, the reaction follows the cross flow pattern. Moreover, such devices have often less trays than distillation columns and thermal effects may be significant. Then taking lateral flow pattern into may become important.

4 MODEL OF A SIDE REACTOR-DISTILLATION COLUMN COMBINATION

4.1 Introduction

Reactive distillation has undisputed benefits in certain applications like in the methyl acetate process (Agreda et al. 1991). However, several aspects limit the applicability of RD. Distillation and reaction must take place at the same temperature and it is known that reaction rates are very sensitive to temperature. On the other hand, temperature is determined by the vapour-liquid equilibrium conditions, thus it can be adjusted in certain limits by modifying the pressure and separation in the column. The operating pressure has an influence on the distillation process. If high pressure is needed for achieving sufficient reaction temperature, efficiency of the separation tends to decrease, column hydraulics tend to deteriorate and the reboiler temperatures may be too high for steam heating resulting in expensive equipment. If temperature should be reduced, low pressure operation results in high volumetric flow rates and large size columns, and a vacuum system or a refrigeration system for the condenser may be necessary

If the RD column is considered as a reactor, a large liquid/catalyst hold-up is necessary. From the reaction point of view free space is disadvantage in the reactor. Distillation in turn needs free space for vapour flow and large mass transfer area. Hold up is not an advantage for distillation.

Finally the catalyst deactivation, which is normally compensated with excess of catalyst or by increasing the reaction temperature or in situ regeneration is impossible in RD columns.

Some of the disadvantages of RD can be relieved and still preserving the benefits of a combined process by considering a Side Reactor Configuration (SRC). See for a schematic process flowsheet of the side reactor process. A liquid side draw from the column is taken and fed into the reactor. The reactor effluent is then returned back into the distillation column. The reactor can be in one phase or a traditional fixed bed catalyst reactor can be used. The adequate catalyst amount is easily arranged in SRC where traditional reactor types and catalyst structures can be used. Also the reaction conditions in SRC are less limited by the distillation requirements, particularly the reaction profile can be optimised.

Combinations of a distillation column and a reactor can be modelled with the standard blocks of a simulation program. However, according to the experience of the author the simulation of the side reactor concept and particularly the optimisation of them is quite tedious with such tools.

Thus developing a dedicated simulation model for SRC system was considered worthwhile. The resulting tool is presented in paper V. The model is implemented in FLOWBAT (Keskinen and Aittamaa, 2004).

4.2 Distillation Stage Model

The target of the modelling was to develop a flexible tool for simulation, design and optimisation of distillation column and side reactor combination.

The model of the distillation column is derived from the mass, and energy balances, equilibrium and summation relations of a stage in a reactive distillation column.. Besides of this basic equation set, a number of specification equations are included. This allows the user to specify for example product purity, temperature, liquid, and vapour flows etc. in the simulation.

Murphree efficiency is included to account for nonideality of the stages. This allows the possibility to the efficiency calculations of various complexities ending up in methods based on multicomponent Maxwell-Stefan diffusion equations

The base of the model was the reactive distillation column model developed by Aittamaa and Kettunen (Kettunen 1988). The part of the model equations pertaining to the distillation column were kept unchanged in as large extent as possible. It should be noted that in this chapter and article IV the suffix j refers to the tray number, whereas in chapter 3 and article III suffix j refers to the number of the mixed pool. This is done in order to maintain the connection to the original articles.
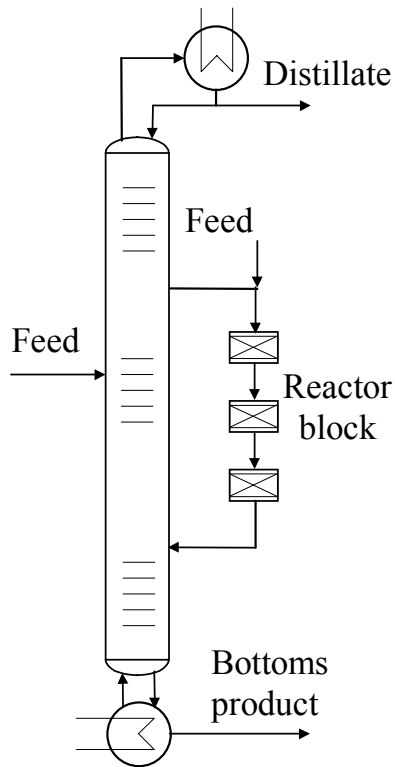
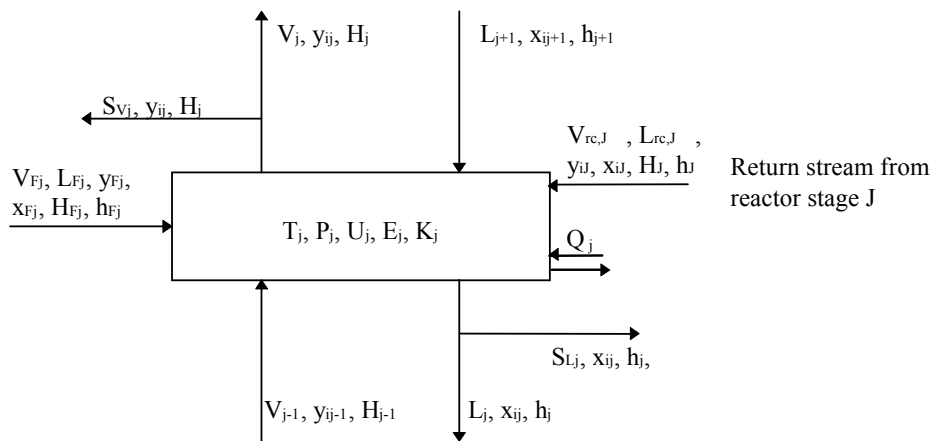Figure 4.1 Schematic flowsheet of a side reactor process

Figure 4.2 Schematic flowsheet of a distillation stage

In this model the independent variables for each distillation tray are:
- n liquid mole fractions
- n vapour mole fractions
- liquid flow rate
- vapour flow rate.
- temperature
- pressure
- heat duty
- liquid phase side draw rate

- vapour phase side draw rate

The corresponding equations to be solved are given below.

The component mass balances n equations for each tray,

$$0 = SKA1 \left(\begin{array}{l} V_{F,j} y_{F,ij} + L_{F,j} x_{F,ij} + V_{rc,j} y_{rc,ij} + L_{rc,j} x_{rc,ij} + V_{j-1} y_{i,j-1} + L_{j+1} x_{i,j+1} \\ + r_{ij} - y_{ij} (V_j + S_{V,j}) - x_{ij} (L_j + S_{L,j}) \end{array} \right) \tag{4.1}$$

Equilibrium relations, the multicomponent , n equations for each tray

$$0 = y_{ij} - \frac{(y_{i,j-1} V_{j-1} + y_{F,ij} V_{F,j})(1 - E_{i,j})}{(V_{j-1} + V_{Fj})} - E_{i,j} K_{i,j} x_{i,j} \tag{4.2}$$

Energy balance, one equation per tray,

$$0 = SKA2 \left(\begin{array}{l} V_{F,j} H_{F,j} + L_{F,j} h_{F,j} + V_{rc,j} H_{rc,j} + L_{rc,j} h_{rc,j} + V_{j-1} H_{j-1} + L_{j+1} h_{,j+1} \\ -H_j (V_j + S_{v,j}) - h_j (L_j + S_{L,j}) + Q_j \end{array} \right) \tag{4.3}$$

Summation equation, one equation per tray,

$$0 = \sum x_{ij} - \sum y_{ij} \tag{4.4}$$

Total mass balance, one equation per tray,

$$0 = SKA1 \left(\begin{array}{l} V_{F,j} + L_{F,j} + V_{rc,j} + L_{rc,j} + \sum r_{ij} + V_{j-1} + L_{j+1} \\ -(V_j + S_{v,j}) - (L_j + S_{L,j}) \end{array} \right) \tag{4.5}$$

The scaling factors are used in these equations, because various equations involve numerically very different quantities. E.g. the enthalpies expressed in J/mol are very different from the molar fractions. When the convergence criteria is the sum of squares of the individual discrepancies, the numerically largest values would become too dominant. In order to equalize the weighing of the discrepancies, the scaling factors are introduced. They are defined:

$$SKA1 = \frac{1}{(1 + L_j)} \tag{4.6}$$

$$SKA2 = \frac{1}{(1 + L_j |h_j| + |Q_j|)} \tag{4.7}$$

for the reboiler (stage 1) the scaling factors are

$$SKA1 = \frac{1}{(1 + V_j)} \tag{4.8}$$

$$SKA2 = \frac{1}{(1 + V_j |H_j| + |Q_j|)} \tag{4.9}$$

These equations add up to $2n + 3$ equations. The additional 4 equations can be chosen from the set of specification equations presented below.

Thus there are $2n + 7$ variables and equations per stage. This is more than in most equilibrium stage models presented in the literature. In those cases stage heat duties and liquid and vapour side draws are not independent variables but their values are specified directly in the input. However, when they are kept as independent variables bound by the specification equations, considerable flexibility of the tray model is achieved. By selecting different specification equations, it is possible to fix other variables of the tray. Currently the following 13 specification equations are available.

Pressure on the stage:
$$0 = \frac{(P_j - P_{j,set})}{(1 + P_{j,set})}$$
(4.10)

Vapour molar side draw:
$$0 = \frac{(S_{V,j} - S_{V,j,set})}{(1 + S_{V,j,set})}$$
(4.11)

Liquid molar side draw:
$$0 = \frac{(S_{L,j} - S_{L,j,set})}{(1 + S_{L,j,set})}$$
(4.12)

Heat duty on stage:
$$0 = \frac{(Q_j - Q_{j,set})}{(1 + Q_{j,set})}$$
(4.13)

Liquid reflux ratio:
$$0 = \frac{(L_j / (S_{L,j} + S_{V,j}) - RD_{L,set}}{(1 + RD_{L,set})}$$
(4.14)

Vapour reflux ratio:
$$0 = \frac{(V_j / (S_{L,j} + S_{V,j}) - RD_{V,set}}{(1 + RD_{V,set})}$$
(4.15)

Liquid composition:
$$0 = \frac{(x_{i,j} - x_{i,j,set})}{(1 + x_{i,j,set})}$$
(4.16)

Vapour composition:
$$0 = \frac{(y_{i,j} - y_{i,j,set})}{(1 + y_{i,j,set})}$$
(4.17)

Temperature:
$$0 = \frac{(T_j - T_{j,set})}{(1 + T_{j,set})}$$
(4.18)

Liquid molar flow:
$$0 = \frac{(L_j - L_{j,set})}{(1 + L_{j,set})}$$
(4.19)

Vapour molar flow:

$$0 = \frac{(V_j - V_{j,set})}{(1 + V_{j,set})} \qquad (4.20)$$

Liquid mass side draw:

$$0 = \frac{(S_{L,j} M_{L,j} - m_{L,j,set})}{(1 + m_{L,j,set})} \qquad (4.21)$$

Vapour mass side draw:

$$0 = \frac{(S_{V,j} M_{V,j} - m_{V,j,set})}{(1 + m_{V,j,set})} \qquad (4.22)$$

Four of these equations can be selected for each tray and the corresponding specification given in input. If pressure, liquid side draw, vapour side draw and heat duty are specified, the specification of the tray is in practice equivalent with that of the most equilibrium stage column models, but as is evident from the list above, other alternatives exist.

4.3 Reactor model

The distillation stage model was the basis of the equation group used to model the reactor segments. A considerable flexibility concerning the structure of the side reactor model could be achieved by maintaining the basic variable and equation system and simultaneously it was possible to take advantage of the extensive work done already for the existing reactive distillation model. Nevertheless, changes were necessary, because most conventional reactors operate in co-current mode rather than in counter-current mode. Provisions for the single phase operation were necessary as well.
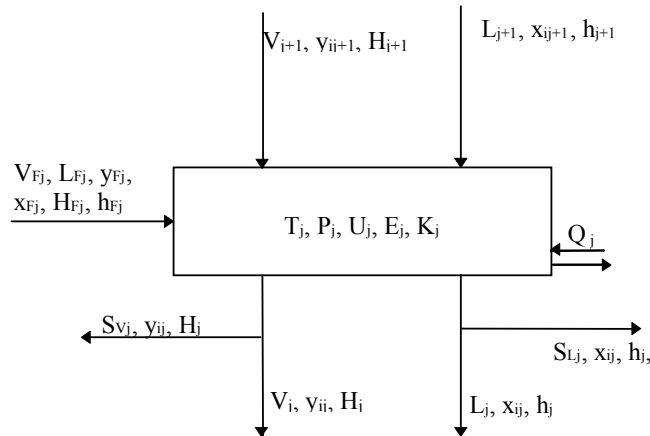

Figure 4.3. Schematic figure of a reactor stage

The component mass balances for the two phase case n equations

$$0 = SKA1 \begin{pmatrix} V_{F,j} y_{F,ij} + L_{F,j} x_{F,ij} + V_{j+1} y_{i,j+1} + L_{j+1} x_{i,j+1} \\ + r_{ij} - y_{ij}(V_j + S_{v,j}) - x_{ij}(L_j + S_{L,j}) \end{pmatrix} \qquad (4.23)$$

The component mass balances for the liquid phase case n equations

$$0 = SKA1\left(L_{F,j}x_{F,ij} + L_{j+1}x_{i,j+1} + r_{ij}^{L} - x_{ij}(L_j + S_{L,j})\right) \tag{4.24}$$

The component mass balances for the vapour phase case *n* equations

$$0 = SKA1\left(V_{F,j}y_{F,ij} + V_{j+1}y_{i,j+1} + r_{ij}^{V} - y_{ij}(V_j + S_{v,j})\right) \tag{4.25}$$

Equilibrium relations, *n* equations

$$0 = y_{ij} - K_{ij}x_{ij} \tag{4.26}$$

The corresponding dummy equations for liquid phase case, *n* equations

$$0 = y_{ij} - \frac{1}{nc} \tag{4.27}$$

The corresponding dummy equations for vapour phase case, *n* equations

$$0 = x_{ij} - \frac{1}{nc} \tag{4.28}$$

Energy balance two phase case

$$0 = SKA2\left(\begin{array}{c} V_{F,j}H_{Fj} + L_{F,j}h_F + V_{j+1}H_{i,j+1} + L_{j+1}h_{i,j+1} \\ -H_j(V_j + S_{v,j}) - h_j(L_j + S_{L,j}) + Q_j \end{array}\right) \tag{4.29}$$

Energy balance liquid phase case

$$0 = SKA2\left(L_{F,j}h_F + L_{j+1}h_{i,j+1} - h_j(L_j + S_{L,j}) + Q_j\right) \tag{4.30}$$

Energy balance vapour phase case

$$0 = SKA2\left(V_{F,j}H_{Fj} + V_{j+1}H_{i,j+1} - H_j(V_j + S_{v,j}) + Q_j\right) \tag{4.31}$$

Summation

$$0 = \sum x_{ij} - \sum y_{ij} \tag{4.32}$$

Total mass balance two phase case

$$SKA1\left(V_{F,j} + L_{F,j} + V_{j+1} + L_{j+1} - (V_j + S_{v,j}) - (L_j + S_{L,j})\right) = 0 \tag{4.33}$$

Dummy equation F5b for the liquid phase case

$$0 = SKA1V_j \tag{4.34}$$

Dummy equation F5c for the vapour phase case

$$0 = SKA1L_j \tag{4.35}$$

As in the distillation stage model the specification equations can be chosen for the reactor stage from an adequate choice of specification equations 4.10 – 4.22.

The resulting equation group for each reactor segment has the same variables and equivalent equations as a distillation stage, but in co-current mode the interactions between segments proceed only to one direction which results in changes to balance equations. Moreover, if the reactor segments are operating in a single phase vapour or

liquid mode, the variables of the missing phase are irrelevant and the phase equilibrium equations are inapplicable. Thus the equilibrium equations are replaced with dummy equations enforcing the concentrations of the missing phase to neutral values. Moreover, in single phase case the total mass balance can be replaced by equation specifying that the total flow rate of the missing phase is zero.

The combined reactor and distillation column model can be used for the simulation of a single distillation column and one sequence of interlinked reactor segments. One basic reactor segment can work as a continuous stirred tank reactor (isothermal or adiabatic). A series of reactor segments can be used to model a fixed bed or tubular reactor. The heat flows or temperature and the pressure can be specified for each reactor segment. A reactor segment can also be specified to work as an intermediate heater/cooler of the stream. Thus such sequence of the reactor segments can represent a rather complex reactor train.

4.4 Method of solution

Since the new SRC model is used as a unit module in a flowsheeting environment including plant optimisation studies, the Newton's solution method was chosen. In solving the linearised subsystem of the model equations a new elimination and back substitution method was developed. The block structure of the Jacobian matrix is shown in figure 4.5.The Jacobian structure and solution method is described in more detail in paper IV.

The Jacobian matrix includes a block tridiagonal part for the distillation column operating in countercurrent mode, a block bidiagonal part for the reactor part operating in co-current mode or single phase mode and two off-diagonal blocks (*D, F*) connecting the two parts together. A special solver was written for the model, designed specifically to take advantage of this Jacobian structure.
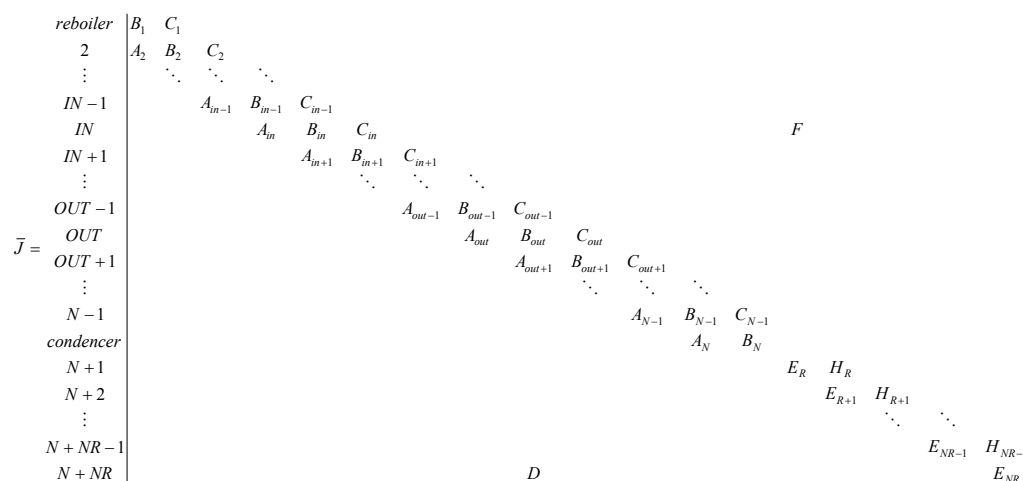

Figure 4.5 The structure of the Jacobian matrix.

The SRC model with the solver developed is implemented to the inhouse simulation program FLOWBAT (Aittamaa and Keskinen, 2004).

The model has certain advantages over a model created by combining distillation column and reactor block(s) of a modular process simulation program. Especially when the reactor block is more complicated than a CSTR e.g. a tubular reactor, the advantages are clear.

If separate modules are used for the modelling, distillation column is solved separately using some of the well established methods and the reactor module is typically solved using an ODE-solver and the connecting streams are matched in an outer iteration loop using e.g Wegstein or Broyden methods. Contrary to this, the SRC module described here solves the whole system with all intermediate streams as a single entity.

The solution of such system consisting of a group of modules is often time consuming and convergence of the recycle streams is frequently difficult. If plug flow reactors are involved, ODE-solver is frequently quite time consuming, compared to the evaluation of the discrepancy equation group and the part of the Jacobian matrix including the reactor equations. Moreover when the system is solved repeatedly with only slightly changed parameter values as is often necessary with the optimisation problems, the intermediate conditions inside the reactor can be easily stored and used as initial values when a new case is solved.

5. APPLICATIONS OF THE SRC MODEL

The performance of the model is demonstrated by examples presented in paper V. In this study the performance of SRC was compared to reactive distillation (RD) in production of several chemicals, including tert-amyl-methyl-ether (TAME) and isobutene dimerization to isooctene.

TAME-production is an example of an equilibrium limited reaction having typically fairly low reaction rates and correspondingly requiring large catalyst volumes. When temperature is increased, reaction rates increase, but the reaction equilibrium becomes less favourable. Thus reactor temperatures and temperature profiles have a strong influence on the performance of the system.

The figure 5.1 presents the conversion achieved with different process alternatives. It is obvious that process based on optimised SRC has superior performance over both the RD system and adiabatic SRC. It is clear as well that adiabatic SRC is inferior to RD at normal reflux ratios. This example clearly illustrates the significance of optimisation.

Qualitatively taken, the optimal temperature profile of the TAME reactors is descending. In the beginning of the reactor train temperatures are optimally high for the higher reaction rates. In the end of the train temperature is lower in order to shift the reaction equilibrium towards the products. Because TAME formation is an exothermal reaction, in an adiabatic reactor the temperature rise towards the end of the reactor and the profile is thus exactly the opposite of the optimal.
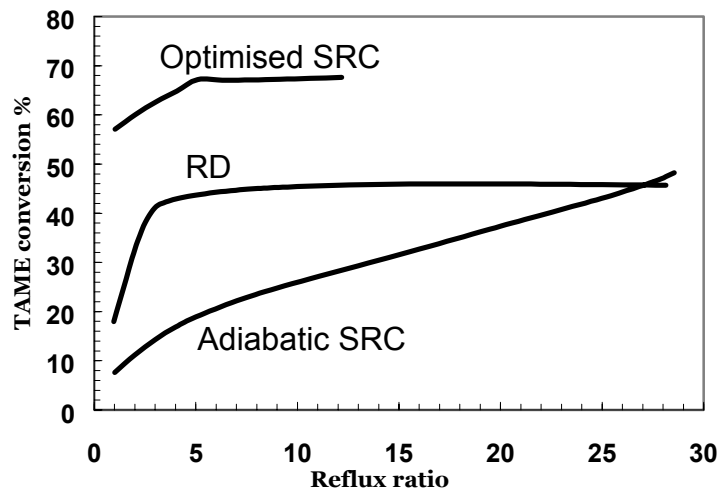
Figure 5.1. Comparison between conversions of reactive distillation, adiabatic side reactor concept and reactor train -optimised side reactor concept. TAME conversion is plotted against reflux ratio. For SRC the reflux flow rate is combined recycle and reflux flow rate.

The isobutene dimerisation process represents a different type of a process. The wanted reaction is irreversible, thus reaction equilibrium is not a limiting factor. However, at high conversions the dimer tends to react further to trimer, tetramer and higher oligomers. Thus conditions must be selected so that an acceptable selectivity is maintained. Thus this system may be considered being limited by the selectivity. For a commercial plant, which has to produce saleable product, the quality requirements are nearly as stringent as any limitation caused by the laws of the nature.

In this case the reaction is exothermal as well. RD is a possible candidate in this case because the reaction products can be removed from the reaction mixture quickly and heat of reaction can be dissipated by the evaporation.

However, SRC competes with RD in this case as well. In SRC the separation of reaction products and recycle of the reactants can be arranged efficiently. Such processes including a SRC part for the olefin dimerization are presented by Aittamaa et al. (2004), Pyhälahti and Aittamaa (2004) and Sloan et al. (2000).

Again the optimised SRC performs better than either adiabatic SRC system and RD, although here the competition is more even. Nevertheless even in this case, in order RD to achieve the conversion of the optimized SRC, a rather high reflux ratio (approximately 4) is needed. Thus the optimised SRC process seems to be the best alternative for real life applications.

The new model performed very well in the optimisation work being fast and reliable.
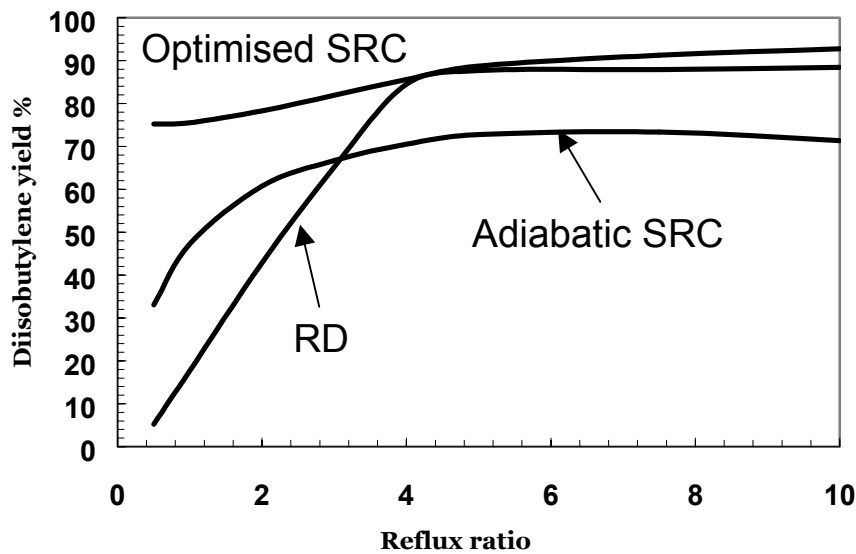
Figure 5.2 Comparison between conversions of reactive distillation, adiabatic side reactor concept and reactor train -optimised side reactor concept. Diisobutylene yield is plotted against reflux ratio. For SRC the reflux flow rate is combined recycle and reflux flow rate.

6. EFFICIENT INTERFACIAL AREA IN ABSORPTION WITH A CHEMICAL REACTION

6.1 Introduction

The actual target of the work was to develop a new plastic tower packing for absorption purposes. Thus, the experimental work was performed in order to compare the performance of the different shapes and the modelling aspects were less important. However, the system used in these experiments is well suited for developing a correlation for the efficient interfacial area and consequently the present correlation was generated.

The part of research made public was just this interfacial area correlation. Paper VI presents the resulting correlations. A more complete presentation of the work done includes to authors licentiate's thesis (Pyhälahti, 1990a).

6.2 Interfacial area correlations in literature

The literature study by Pyhälahti (1990b), revealed that there is a large number of different mass transfer correlations for packed beds, e.g Schulmann et a..1955, Onda et al. (1967), Kolev et al. (1976), Linek et al (1984), Shi and Mersman (1984) have presented correlations for the efficient interfacial area of the packed beds. After the making that study, e.g. Billet and Schultes (1993), Hanley et al. (1994) and Linek et al. (2001) have published such correlations for random packing. There is a significant variation in the

predictions of the influence of the the various properties of the system to the resulting mass transfer rate.

One very clear trend in the evolution of tower packing types has been proceeding towards more and more open shapes, consisting of lattice-like structures instead of relatively large smooth surfaces. Schultes (2003) presents a genealogy of the tower packing types, which makes this point very clear. First specially fabricated random packing was the Raschig ring and in 1930s the Berl saddle was introduced. In early 1950s the Intalox saddle appeared to compete with the Berl saddle. About the same time basic ring shape was modified by cutting openings to the packing walls. The result was so called Pall-ring. The ring shape was preserved, but the packed bed as a whole had much more open structure because the openings provided the access to the inside of the packing pieces. In 1970s the new packing shapes like IMTP and Nutter ring were introduced. Their shape resembles only very vaguely the traditional rings or saddles. In late 1990s was presented Raschig Super-ring, which consists entirely of some narrow interconnected stripes of metal. Thus, the development towards more open structure consisting of more and more narrow stripes is clear.

The results presented e.g. by Schultes (2003) show how the pressure drop at given flow rate is strongly reduced and the height of the mass transfer unit remains about constant in comparison between Pall ring, IMTP, Nutter ring and Raschig Super-Ring. This is a surprising result considering that reduction of pressure drop is likely to result in lower intensity of turbulence in the gas phase and thus lower gas side mass transfer coefficients. One possible explanation is that the vapour and liquid phases have better access to each other, i.e. the efficient interfacial area is larger although the packed beds have nearly the same specific geometric area.

Linek et al. (2001) have studied the RSMR packing of 20 40 and 50 nominal size. The authors measured gas and liquid side mass transfer coefficients and the interfacial area. Interfacial area measurement was done using the very same procedure than in this work, i.e. CO_2 absorption to aqueous NaOH-solution. According to the graphs given by the authors, the measured ratio of the interfacial area to the geometric area of RSMR rings is consistently higher than that of Pall rings measured earlier by Linek et al. (1995).

The geometric factors included to the most correlations for the specific surface area are the geometric specific surface of the packed bed and some linear dimension of the packing itself. Most popular linear dimension is the nominal size of a packing piece. Some authors have used the diameter of a sphere having same surface area than a single piece of the packing.

Both these linear dimensions are strongly correlated to the specific surface area of the bed. Considering packing of a certain shape, the specific surface area of the bed is inversely proportional to the diameter of a single piece of packing as a simple geometrical consideration shows. Moreover, packing types having very different geometries tend to have surprisingly similar specific surface areas, e.g 50 mm Pall-rings, Nutter rings, IMTP and Raschig Super-rings all have specific geometric area of about 100 m^2/m^3 according to Schultes (2003) and Linek et al. (2001). Also 50 mm metal Raschig rings have the same specific surface area. Thus using nominal diameter as linear dimension brings very little additional information to the correlation over the specific surface area of the bed.

Many correlations take the geometry of the packing into account by involving coefficients specific to each shape. This is a viable method and avoids the problem of creating theories about badly known phenomena, but results in correlations which cannot be extended beyond the shapes for which the experimentally determined parameters are available.

One phenomenon very little researched but very important in practice is the precipitation of solids on the packing surfaces. Recently e.g. Groberichter and Stichlmair (2003) have studied the deposition of the inorganic salts on various packings and their results show that under suitable conditions very considerable depositions of inorganic salts may occur. In their study the purpose was to study the effect of such deposits on the hydraulic performance of the bed but it illustrates the probable deposition mechanism, precipitation of the salt from saturated solution due to evaporation of the solvent.

The wettability of the packing has strong influence on the mass transfer performance as is clearly illustrated by the study of Linek et al. (1984) where plastic Pall rings were tested as received from manufacturer and after hydrophilisation treatment. The efficient interfacial area increased clearly with improved wettability.

Considering the results of Groberichter and Linek together, gives an interesting idea about the possible influence of minor amounts of inorganic impurities on the performance of plastic packings. If the deposition is not so heavy that it has a negative influence on the hydraulics of the packed bed, a thin film of inorganic impurities may give similar performance enhancement as is shown by the results of Linek et al. (1984) without any specific treatment. The experiments of Groberichter (2003) show that e.g. evaporation of the solvent from nearly saturated salt solution may lead to precipitation of the inorganic material over the whole height of the packed bed, at least if the bed is not very tall.

6.3 Packings studied

Some of the experimental types tested are shown in figure 6.1. Because of the flat shape of the packing pieces, they prefer horizontal position when dumped to the column. These packing are continuously manufactured with the name HUFO.
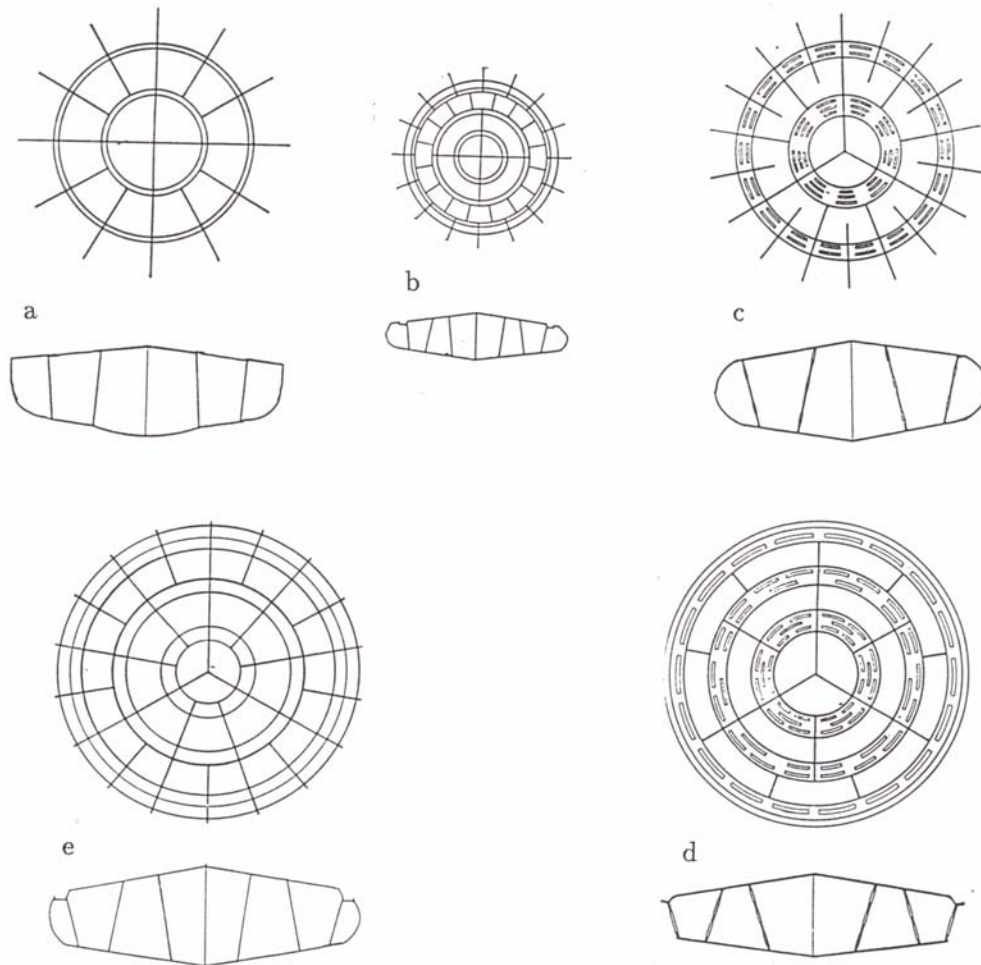
Figure 6.1. The various shapes of HUFO packing used in experiments.

6.3 Experiments

The selection of the experimental system was dictated by the fairly large size of the equipment due to the large size of the packing to be tested.

The smallest type which was originally thought to be the most relevant type for absorption columns, had diameter of 0.07 meter and the diameters of the other types was between 0.13 and 0.155 meter. The smallest type was originally though to be the most appropriate for absorption columns because of it's high surface area. However later the larger types proved to be more interesting.

The experimental system selected was absorption of carbon dioxide from air (approximately mole 1 %) to approximately 1 M sodium hydroxide solution. The absorbed carbon dioxide reacts with sodium hydroxide according to the formula:

$$CO_2 + 2\ NaOH(aq) \leftrightarrow Na_2CO_3\ (aq) + H_2O$$

This is a fast reaction with reaction taking place in the liquid film. Dankwerts (1970) has shown that the local mass transfer rate in this system is determined in practice by the rate of the chemical reaction and the flow conditions have little influence on it. Thus the point mass transfer flux can be estimated from theory and the efficient interfacial area can then be calculated from the total mass transfer rate.

In this work, the shape and properties of the packing involved were such that the overall diameter seemed especially ill suited basis for the correlation. Thus it was made a simple trial to find some other linear dimension than the packing nominal size and to use that for correlating the results.

The wettability of the packing surface is another important factor for the resulting efficient interfacial area. Its importance is easy to understand on a qualitative level and many of the correlations include a parameter describing the wettability of the packing surface. However, controlling all factors affecting the wetting of the packing surface is difficult. The wetting properties of surfaces depend on surface phenomena, which may be altered by very low concentrations of surface active agents, or by tiny amounts of substances deposited on them. The effect of the latter factor was detected in our experiments, thus, contact angle of the surface was included to the correlations as a factor describing the wettability of the packing surface.

The functional form of the correlation was based on the results of the literature study and dimensional analysis. The general forms selected were:

$$a_e d = K_1 Ga^a \operatorname{Re}^b (\cos\theta)^c \qquad (6.1)$$

and

$$a_e d = K_2 Ga^a \operatorname{Re}^b (\cos\theta)^c + K_3 \qquad (6.2)$$

where:

$$Ga = \frac{d^3 g \rho_L^2}{\eta_L^2} \text{ , Galilei number, dimensionless}$$

$$\operatorname{Re} = \frac{Ld}{\eta_L} \text{ , Reynolds number, dimensionless}$$

a_e = efficient interfacial area, m2/m3
$\cos\theta$ = cosin of the contact angle, dimensionless
d = characteristic dimension, m
a,b,c = constants, dimensionless
$K1$, $K2$, $K3$ = constants, dimensionless

The form of the equation (1) represents the most usual functional form applied in chemical engineering, i.e. product of power functions of the parameters. The literature study revealed that the actual measured data does frequently not follow on path going smoothly through the origin as such a function would implicate. Thus it was thought worth of trying also function involving a sum term, i.e. equation (2).

The packing overall diameter (d_t in following tables), inverse of the specific surface of the packed bed, the efficient width of the surface elements (d_{eff} in following tables),and an

dummy constant dimension were tried in different combinations. Table 6.1 presents the values of each parameter in equations 6.1 and 6.2 for each characteristic dimension.

These correlations are dimensionless. The previously mentioned width of surface elements was included to the characteristic dimension d, which has the dimension of length. In many cases the diameter or nominal size of the packing has been used for this purpose. If packings of uniform shape with different sizes are compared, there is no difference between the width of the surface elements or nominal size, because in such case they are directly connected. The differences occur when packings with different shapes are compared. Another possibility is to use inverse of the specific surface of the packed bed. That was tried here as well, but the best result was achieved with the width of the surface elements.

Table 6.1 Values of the parameters in equation 6.1 for various definitions of the characteristic dimension

d	K_1	a	b	c	m_σ
1.0 m	0.09133	0.1488	0.2746	2.222	8.488
d_t	0.1085	0.1107	0.3059	2.575	6.886
a_t^{-1}	0.005096	0.2504	0.2730	2.285	8.619
$d_{eff}^{0.25} a_t^{-0.75}$	0.01057	0.2033	0.2779	2.267	8.052
$d_{eff}^{0.5} a_t^{-0.5}$	0.03573	0.1282	0.2872	2.357	7.128
$d_{eff}^{0.75} a_t^{-0.25}$	0.09320	0.07227	0.2977	2.552	6.329
d_{eff}	0.1192	0.06138	0.3033	2.728	5.932

Table 6.2 Values of the parameters in equation 6.2 for various definitions of the characteristic dimension

d	K_2	a	b	c	K_3	m_σ
1.0 m	0,01173	0,1774	0,3848	3,077	17,42	8,468
d_t	0,1094	0,1105	0,3056	2,573	-0,0078	6,885
a_t^{-1}	$0,6160 \cdot 10^{-6}$	0,7371	0,5180	5,256	0,2772	7,274
$d_{eff}^{0.25} a_t^{-0.75}$	$0,5866 \cdot 10^{-8}$	0,9920	0,5735	5,752	0,3455	7,235
$d_{eff}^{0.5} a_t^{-0.5}$	$0,1135 \cdot 10^{-6}$	0,7979	0,5439	4,870	0,3728	7,150
$d_{eff}^{0.75} a_t^{-0.25}$	0,01240	0,1526	0,3960	3,386	0,2205	6,349
d_{eff}	0,02827	0,1140	0,3796	3,401	0,2064	5,954

The results achieved with the form of equation (1) are considered more interesting and are discussed here. From the definitions of the dimensionless groups and the equation (1) can be seen that all other factors being constant, the efficient interfacial area is proportional to the characteristic dimension as

$$a_e \propto d^{3a+b-1} \tag{6.3}$$

When the correlated value of Galilei number exponent a is 0.0614 and that of Reynolds number exponent b 0.303, it can be seen that the efficient interfacial area is predicted to be proportional to the width of surface elements as:

$$a_e \propto d^{-0.51} \tag{6.4}$$

When specific surface area of the bed a_t was used as the basis of the correlation, the exponent values were changed as well. Then a was 0,250 and b was 0.273. In that case:

$$a_e \propto a_t^{0.02} \tag{6.5}$$

Thus increasing the specific surface of the bed has a very small effect on the correlated efficient interfacial area.

When results were correlated using the particle overall diameter, the result was

$$a_e \propto d_p^{-0.34} \tag{6.6}$$

The resulting sum of the squares of the deviations was slightly larger than with the correlation using width of the surface elements as basis. That the results are near each other is not surprising, because even if the packings involved were of very different shapes, the width of surface elements was nevertheless strongly correlated with the overall size of the packing. There was a significant difference between experimental packing types having perforations and not having perforations and thus the number of experimental points really showing the wanted effect was less than half of all measurements.

Another result was that during repeated experiments a thin hydrophilic layer was deposited on the surface of the packing. This film improved the mass transfer performance substantially by approximately doubling the effective interfacial area under the experimental conditions.

6.4 Conclusions

A set of correlations of the efficient interfacial area of plastic tower packings was developed. The correlations are general in that respect that they are not bound to any specific packing shape. Moreover, the correlations make an attempt to introduce a general geometric parameter, which would improve the mass transfer correlations with the modern random packing having a lattice like structure against the traditional shapes consisting of fairly large continuous surfaces. This development towards structures consisting of thinner and thinner basic elements has been ongoing for decenniums, thus one would assume that the packing performance has indeed been improved as a result of such modification.

Nevertheless, not any generalized correlation for random packing published has made an attempted to introduce any general parameter describing this structural property of the packing. The geometric parameters applied have been the overall size and specific area. The usual way to take the varying geometry of different packing types into account has been to introduce specific parameters, which are fitted to the experimental results and are valid only to the specific packing shape for which they are determined.

The correlations presented here make at least an attempt to take a more general approach. The width of the surface elements is used as a geometric parameter. It is defined in the article VI and a method for evaluating it for new shapes is presented as well.

It is clear that the proposed method of taking into account one factor having influence on the efficient interfacial area is very rudimentary and taking full advantage of it would require additional experiments including more different types of packing. However, correlating the efficient interfacial area using width of the surface elements as the characteristic dimension of the packing gave better results than diameter of the packing or inverse of the bed specific surface. Taking into account that tower packing is used as a bed and not as single pieces, it is understandable that the overall dimension of single packing piece is not necessarily the best possible basis of correlation. Especially with packing consisting of large pieces of relatively complex shape, the overall bed geometry may be badly described by the maximum dimension of the packing.

For the purposes of this study, it had been very interesting to have very different types of packing in the experiments, e.g. saddles and packing consisting of thinner basic elements.

Another highly interesting finding of practical importance was that the wettability of plastic packing was dramatically improved due to impurities present in the mixture without any troublesome chemical treatment which e.g. Linek et al. (1984) applied. During the repeated test runs with a same lot of packings a small amount of polar impurities was deposited on the packing surfaces. A possible mechanism was that calcium carbonate present in tap water was precipitated on packing surfaces when water was evaporated from the solution to the air flow through the column. The formation of this hydrophilic layer was enough to more than double the efficient interfacial area of the packed bed.

As such it is well known that the hydrophobic plastic packing perform worse than metallic or ceramic packing in experiments made with aqueous solutions. However, this finding indicates that in real processes where solutions seldom are really clean and operation is continuous, it is possible that after some time the plastic packing has a hydrophilic layer on its surface without any special treatment. Thus plastic packings may performs better than expected.

7. CONCLUSIONS

7.1 Model Based Process Development

A TAME manufacturing process based on RD was set up and tested successfully in pilot scale. The process was set up on the basis of kinetics and VLE data measured in laboratory with batch and CSTR reactors but without any preliminary experiments in actual RD columns. The tool used was an equilibrium stage reactive distillation model (Kettunen, 1988). These tests clearly show the power of modelling in the process development work.

The pilot tests verified the existence of the expected operating regimes and the general behaviour of the system. Reactive distillation was proofed to be an interesting alternative when the reaction is strongly equilibrium limited. In such case the once trough conversion is not high enough and a combination of reactor and separator system must be considered.

However, the contradiction between the large catalyst hold-up and high residence times required by the reaction and the large vapour space required by the distillation diminishes the applicability of RD. There are additionally well-known limitations of RD, like the narrow operating window and difficulties with the catalyst inside the column.

In TAME production it was finally found that the equilibrium limitation of the reaction was not too serious but the necessary catalyst volume was an acute problem. Thus the final process commercialised as NExTAME process by Neste Oy was based rather on SRC than RD approach.

7.2 Modelling of reactive cross flow trays

The rate-based approach in its basic implementation, does not take into account the composition gradients evolving on large distillation trays. Two alternative models to take this into account were developed. The first one presented above in chapter 3.2 is an addy diffusion model. The second one is a mixed pool model presented in chapter 3.3. A special feature of the mixed pool model is that it can treat efficiently into account the various vapour mixing conditions.

The traditional way to model a distillation column is to use the so-called equilibrium stage model. In actual operation the distillation plates rarely behave as an equilibrium stage. It has been found experimentally that the plate efficiencies often vary in various column sections and in multicomponent systems even each component has individual plate efficiencies that deviate from component to component.

Two main approaches are available to calculate the real separation of a distillation column. In the first procedure binary NTU:s (number of transfer units) are first estimated for all components. Then Murphree point efficiencies are calculated from these NTU:s using the two-film theory and the Maxwell-Stefan equations. For large plates mixing models for liquid and vapor flows on the plate are used to obtain the plate efficiencies (sf. Ilme 1997).

Another approach is the rate-based approach (sf. Taylor and Krishnamurthy, 1985a, Taylor et al., 1994) where the heat and mass transfer including multicomponent interactions between the components are directly calculated using heat and mass transfer coefficients on the plate. In this approach, the film theory and the Maxwell-Stefan equations for diffusion are applied, too.

However, the rigorous the eddy diffusion model had not been applied rigorously to solving a reactive distillation problem. The same applies to the mixed pool model other vapour mixing cases than total mixing between the stages.

These model were implemented to the RD simulation program DESIGNER. This RD tool is based on the rate-based approach, and can handle a large spectrum of reactions (homogeneous and heterogeneous; slow, average and fast; equilibrium and kinetically controlled), reactions in both bulk and film phases are accounted for, different hydrodynamic models and a large choice of hydrodynamic and mass transfer correlations for various types of column internals (trays, random and structured packing, catalytic packing) are implemented in the code. The simulation results obtained by this program have been published also for MTBE production and ethyl acetate synthesis by reactive distillation by Kenig et al. (1999) and Kenig et al. (2001).

When considering simulations with the mixed pool model it was shown with a MTBE production example that the change of concentrations over a tray is significant in comparison to the difference between adjacent trays. However, in a reacting system the final difference between both the eddy diffusion and mixed pool models and otherwise identical rate based model but assuming completely mixed liquid phase, was small. The probable reason is that in a relatively tall distillation column there is rarely such huge concentration difference over a single tray that the effect of its concentration profile on the overall performance of the column would be significant. MTBE-formation is a reaction where conversion is limited by equilibrium and tends to compensate the changes as well.

The same way, the results involving vapour plug flow model are rather near to each other, but both differ somewhat more from the results achieved with the mixed vapour model. Thus it seems that in this case the method used for calculating the local mass transfer rate is more important than the tray scale hydrodynamic model. Also when the effect of the vapour flow pattern from plate to plate was tested, the results differ from the mixed vapour case very little.

In a short column with high heat of reaction the situation is different. In this case the resulting rate of reaction with complete liquid mixing gave overall reaction rate 1.3 mol/s whereas the same problem solved using mixed pool model gave overall reaction rate of only 0.7 mol/s. The calculations showed large variation of the internal liquid streams of the column due to the heat of reaction. The example could be relevant to industrial practice for short columns involving high thermal effects. This kind of equipment could be for example a reactive absorber. They are often used for highly exothermal systems and moreover, they have frequently rather small number of stages.

These examples shows that there are still interesting aspects to study in the operation and design of a RD column. If a cross flow operation is considered the composition gradients and the behaviour of the reaction is also dependent of the reaction type. An equilibrium reaction like the MTBE reaction and an irreversible consecutive reaction (Higler et al.

1999b) have different demands on the structures and flows of the tray. The models presented in this study make possible to estimate the effect of cross flow pattern before the actual column is built. That information is practically impossible to achieve with reasonably sized pilot equipment, because in small columns the liquid mixing is essentially complete.

7.3 Modelling of reactive separation processes

In many applications the Side Reactor Concept (SRC) or a combination of conventional reactor and a distillation column is a remarkably efficient solution. In such system a side draw from the column is taken and fed into a reactor and the reactor effluent is then returned back to the distillation column. As part of this study a dedicated tool for simulating SRC was developed. The model was based on earlier RD model (Kettunen, 1988).

The SRC model was implemented as a module in a unit modular flowsheet simulator. A very versatile reactor model was developed based on the equilibrium stage RD column model. The equations were solved simultaneously with Newton's method. A new efficient elimination and backsubstitution algorithm was developed for the equation group evolving from the SRC process.

The developed software tool is flexible and open allowing easy adaptation to various process configurations and process conditions. The implementation of the model is done into the flowsheeting software FLOWBAT.

7.3 Modelling of efficient interfacial area of tower packing

In this study was developed an experimental correlation for plastic random packings manufactured under the name HUFO. The method used for efficient interfacial area was chemical absorption of carbon dioxide from air to aqueous sodium hydroxide solution.

The developed correlation differs from other efficient interfacial area correlations published by taking into account the structure of the packing by introducing the width of the packing surface elements into the correlation. This clearly improved the agreement between the predicted and measured efficient interfacial areas.

REFERENCES

Aittamaa, J., Jakkula, J., Lindqvist, P., Koskinen, M., Linnekoski, J., Krause, O., Sourander, M., Ignatius, J., Pyhälahti, A., 2003, Process for producing a fuel component, US 6,613,108 (B1), Acc 2.9. 2003, 23 p.

Alejski, K., 1991, Computation of the Reacting Distillation Column Using a Liquid Mixing Model on the Plates, *Comput. Chem. Eng.* **15**, 313.

Alejski, K. Szymanowski, J., Bogacki, M., 1988, The application of a minimization method for solving reacting-distillation problems, *Comput.Chem.Eng.* **12**, 833-839.

Ashley, M.J. and G. G. Haselden, 1970, The calculation of plate efficiency under conditions of finite mixing in both phases in multiplate columns, and the potential advantage of parallel flow, *Chem. Eng. Sci.* **25**, 1665-.

Grosserichter, D., Stichlmair, J., 2003, Crystallization fouling in packed columns, Trans IChemE **83**, Part A, 68-73.

Higler, A., Krishna, R., Taylor, R., 1999a, Nonequilibrium cell model for multicomponent (reactive) separation processes, *AIChE J.* **45**, 2357-2370.

Higler, A. P.; Taylor, R.; Krishna, R., 1999b, The influence of mass transfer and mixing on the performance of a tray column for reactive distillation, *Chem. Eng. Sci.* **54**, 2873-2881.

Hung, J-S. 1991, A second generation nonequilibrium model for computer simulation of multicomponent separation processes., Ph,D.Thesis, Clarckson Univ.

Ilme, J., 1997 Estimating plate efficiencies in simulation of industrial scale distillation columns, *Lappeenranta University of Technology, Research papers* 57, Ph.D. Dissertation.

Kenig, E. Y., H. Bäder, A. Gorak, B. Bessling, T. Adrian, and H. Schoenmakers, 2001, Investigation of Ethyl Acetate Reactive Distillation Process, *Chem. Eng. Sci,* **56**, 6185.

Kenig, E. Y. and Górak, A. 1995, A film model based approach for simulation of multicomponent reactive separation, *Chem. Engng Process.* **34**, 97-103.

Kenig, E., Jakobsson, K., Banik, P., Aittamaa, J., Gorak, A., Koskinen, M., Wettmann, P., 1999 An integrated tool for synthesis and design of reactive distillation, *Chem. Eng. Sci.* **54**, 1347-1352.

Keskinen, K.I., Aittamaa, J., eds., 2004, FLOWBAT, User's Instruction manual, Helsinki University of Technology, Laboratory of Chemical Engineering and Plant Design, Espoo,.

Kettunen, M., Tislauksen mallitus, kun reaktio tapahtuu kolonnissa, 1988, Ms. S. Thesis, Helsinki University of Technology, Laboratory of Chemical Engineering and Plant Design, Espoo, Finland. (in finnish).

Kolev, N., Wirkungsweise von Füllkörperschüttungen, 1976, *Chem. Ing. Tech*, **48,** 1105--1112.

Kooijman, H.A., Taylor, R., A nonequilibrium model for dynamic simulation of tray distillation columns*, AIChE J.* **41** (1995) 1852-1863.

Krishnamurthy, R., Taylor, R., 1985a, A nonequilibrium stage model of multicomponent separation processes. Part I: model description and method of solution, *AIChE J.* **31**, 449-445.

Krishnamurthy, R., and Taylor, R., 1985b, A nonequilibrium stage model of multicomponent separation processes. Part II: comparison with experiments, *AIChE J.* **31**, 456-465.

Krishnamurthy, R., Taylor, R., 1985c, A nonequilibrium stage model of multicomponent separation processes. Part III: the influence of unequal component efficiencies in process design problems, *AIChE J.* **31**, 1973-1985.

Krishnamurthy, R., Taylor, R., 1985d, Simulation of packed distillation and absorption column, *Ind. Eng. Chem. Proc. Des. Dev.* **24**, 513.

Krishnamurthy, R., Taylor, R., 1986, Absorber simulation and design using a nonequilibrium stage model, *Can. J. Chem. Eng.,* **64,** 1976-.

Lewis, W. K., Rectification of binary mixtures, 1936, *Ind.Eng.Chem.*, **28**, p. 399.

Lindqvist, P., Järvelin, H., Tamminen, E., Koskinen, M., Aittamaa, J., 1996, NExTAME Process Development, *Proceedings, of The Second Nordic Symposium, on Reactive Separation Systems*, Helsinki University of Technology, Espoo, 129-140.

Linek, V., Petricek, P., Benes, P., Braun, R., 1984, Effective interfacial area and liquid side mass-transfer coefficients for columns randomly packed with hydrophilised and untreated plastic packings, *Chem. Eng. Res. Des.*, **62**, 13--21.

Linek, V., Sinkule, J., Brekke, K., 1995, *Chem. Eng. Res. Des,.* **73**, Part A 398.

Muller, N.P., Segura, H., 2000, An overall rate-based stage model for cross flow distillation columns, *Chem. Eng. Sci.* **55**, 2515.

Onda, K., Takeuchi, H., Okumoto, Y., 1968, Mass transfer coefficients between gases and liquid in packed columns, *J. Chem. Eng. Japan*, **1**, 56-62.

Onda, K., Takeuchi, H., Koyama, Y., 1967, Effect of packing materials on the Wetted surface area, *Chem. Eng. Jpn*, **31**,126—134

Powers, M.F., Vickery, D.J., Arehole, A., Taylor, R., 1988, A nonequilibrium stage model of multicomponent separation process -V. computational methods for solving the model equation, *Comp.Chem.Eng* **12**, 1229-1241.

Pyhälahti, A., Järveläinen M., 1990, Correlations of the liquid side mass tranfer coefficient and interfacial area in packed columns, paper in CHISA '90 conference, 11 p.

Pyhälahti A., Reactive Distillation in Literature, *Plant Design Report Series*, Report No. 42, Helsinki University of Technology, Espoo 1996, 108 p.

Pyhälahti A., Korrelaatio täytekappalekerroksen teholliselle pinta-alalle, *Licentiate's Thesis*, Helsinki University of Technology, Espoo 1990, 72 p.

Pyhälahti, A. Aittamaa, J., 2003, Process for dimerizing light olefins to produce a fuel component, US 6,660,898 (B1), Acc 9.12.2003, 8 p.

Rihko, L.K., Kinnekoski, J.A., Krause, O.A.I., 1994, Reaction equilibria in the synthesis of 2-methoxy-2-methyl-butane and 2-ethoxy-2-methyl-butane in the liquid phase, *J Chem Eng Data*, **39**, 700-704.

Rihko, L.K., Kiviranta-Pääkkönen, P.K., Krause, O.A.I., 1996, Kinetic model for the etherification of isoamylenes with methanol, *Ind Eng Chem Res*, **36**, 614-621.

Shi, M.G., Mersmann, A., 1983, Effective Interfacial area in packed columns, *German Chem. Eng.*, **8,** 87--96.

Shulman, H.L., Ullrich, C.F., Proulx, A.Z., Zimmerman, J.O., 1955, Performance of packed columns II, Wetted and interfacial areas, Gas- and liquid phase mass transfer rates, *AIChEJ* , **1,** 253--258.

Sloan, H.D., Birkhoff, R., Gilbert, M.F., Pyhälahti, A., Nurminen, M., NPRA 2000 Annual meeting, AM-00-34.

Taylor, R., Krishna, R., *Multicomponent mass transfer*, John Wiley, New York 1993.

Taylor, R., Krishna, R., Modelling reactive distillation, *Chem. Eng. Sci.* **55** (2000) 5183-5229.

Taylor, R.; Kooijman, H. A.; Hung, J. S., 1994, A second generation nonequilibrium model for computer simulation of multicomponent separation processes, *Comp. Chem. Eng.* **18**, 205-217.

NOTATION

a,b,c	constants, dimensionless
a_e	efficient interfacial area, m2/m3
C	Vapor flow between the mixed cells in mixed pool model, mol/s
c_t	molar concentration, mol/m^3
D_e	eddy diffusion coefficient, m^2/s
$\cos \theta$	cosin of the contact angle, dimensionless
$Ga = \dfrac{d^3 g \rho_L^2}{\eta_L^2}$	Galilei number, dimensionless
$Re = \dfrac{Ld}{\eta_L}$	Reynolds number, dimensionless
d	characteristic dimension of the packed bed, m
G	Gas flow rate in section 3.1
g	acceleration in the gravity field of earth, 9.80665 m/s^2
L	Feed rate, mol/s
h_f	height of the froth on the tray, m
H^L	molar enthalpy liquid, J/mol
H^V	vapour enthalpy, J/mol
$\mathbf{N'}(l)$	mass transfer rate vector per unit length at location l, mol/(m s)
N_i'	mass transfer rate of component i per unit length, mol/(m s)
$\mathbf{R'}(l)$	reaction rate vector per unit length , mol/(m s)
R_i'	reaction rate of component i per unit length, mol/(m s)
$E'(l)$	heat transfer rate per unit length at location l, W/m.
$K1,\ K2,\ K3$	correlation constants, dimensionless
l	distance from exit weir of the tray along the flow path, m
l_f	distance of the inlet weir from the exit weir along the flow path, m
L	Liquid flow rate, mol/s
n	number of components
p	pressure, Pa
u	number of mixed pools
S	Side draw rate, mol/s
V	vapour mole rate, mol/s
w	Width of the flow path, m
$\mathbf{x}$	Vector of liquid mole fractions
y_i	vapour mole fraction
x_i	Liquid molar fraction of component i

Greek letters

η	Viscosity, kg/ms
ρ	density, kg/m^3

Subscripts

i	component

j	mixed pool in section 3, stage number in section 4
k	tray index in section 3
L	liquid
V	vapour